INSTITUTO SUPERIOR DE ENGENHARIA DE LISBOA

Área Departamental de Engenharia de Electrónica e Telecomunicações e de Computadores

Improvements Towards a More Realistic LoRa Network Simulator

Sérgio David Santos Rodrigues Marques Francisco

Licenciado

Dissertação para obtenção do Grau de Mestre
em Engenharia de Electrónica e Telecomunicações

Orientadores : Prof. Doutor Pedro Renato Tavares Pinho
Prof. Doutor Nuno Miguel Abreu Luís

Júri:

Presidente: Prof. Doutor Nuno Cruz

Vogais: Prof. Doutor Ricardo Marques Correia
Prof. Doutor Pedro Renato Tavares Pinho

March, 2021

INSTITUTO SUPERIOR DE ENGENHARIA DE LISBOA

Área Departamental de Engenharia de Electrónica e Telecomunicações e de Computadores

Improvements Towards a More Realistic LoRa Network Simulator

Sérgio David Santos Rodrigues Marques Francisco

Licenciado

Dissertação para obtenção do Grau de Mestre
em Engenharia de Electrónica e Telecomunicações

Orientadores : Prof. Doutor Pedro Renato Tavares Pinho
Prof. Doutor Nuno Miguel Abreu Luís

Júri:

Presidente: Prof. Doutor Nuno Cruz

Vogais: Prof. Doutor Ricardo Marques Correia
Prof. Doutor Pedro Renato Tavares Pinho

March, 2021

"You never fail until you stop trying."
— Albert Einstein

Acknowledgments

First I would like to thank my thesis supervisors, Professor Pedro Renato Tavares Pinho and Professor Nuno Miguel Abreu Luís for all their support and guidance throughout the development and writing of this dissertation. To them my sincere thank you.

I would like to thank Instituto Superior de Engenharia de Lisboa (ISEL) and all the people - professors and peers - that contributed in some shape or form along the way up until this point. It truly was a second home.

I would also like to thank Instituto de Telecomunicações (IT) for the support and conditions provided during the writing of this work.

And last but not the least, I would like to thank my family, friends and specially my girlfriend Mariana, for their unconditional support and encouragement throughout my years of study and writing of this dissertation, specially during times where doubt and tiredness seemed to take the best of me. Thank you for your support, without you this accomplishment would not be possible.

Abstract

Under the scope of Smart Cities, Low Power Wide Area Networks (LPWANs) have been seen as one of the enabling technologies for the data gathering process in different scenarios, namely in large-scale. However, the methodology used to ascertain the quality and viability of different real type scenarios can prove to be demanding and sometimes nearly impossible to emulate. This necessity urged the development of simulators for different types of Internet Of Things (IoT) networks.

This dissertation addresses the development of a simulator for Long-Range (LoRa) networks, studying the impact that the propagation and capture-effect models have in such networks. This simulator uses some of the development done on the LoRaSim, but it differentiates itself by having the capacity to set up networks with greater detail, allowing the use of different parameters - Spreading Factor (SF), Bandwidth (BW), Code Rate (CR) and payload - in the devices on the network and by having an external network planning module. Multiple analysis are done to different type of networks (small/large-scale, one/multiple gateways) to learn the impact of the devices choice and gateway placement in the network quality.

The results obtained show that both models (propagation and capture-effect) used in LoRaSim are too simplistic, leading to results that fall short of what is expected on real-world scenarios. When an urban environment oriented propagation model (Okumura-Hata) is used with a more realistic capture-effect model in a network that promotes heterogeneity by using devices with different characteristics, the simulator becomes more realistic and therefore - since both models that were used originally were not adequate and were too much pessimistic - the network quality improves significantly.

Keywords: LoRa networks, network planning, propagation model, capture-effect,

performance evaluation

Resumo

As redes de *Internet of Things (IoT)* têm sido vistas como uma tecnologia com grande potencial para resolver alguns dos problemas existentes na sociedade (como por exemplo: optimização de recursos energéticos, monitorização de niveis de poluição atmosférica e até previsões de mudanças climatéricas). Com o avançar da ciência e dos anos, o aumento do número de dispositivos autónomos ligados a redes IoT tem vindo a aumentar consideravelmente. Estes dispositivos são úteis em diversas áreas (comunicações, energia, transportes, saúde entre outras), contudo, seja qual for a utilização dada aos dispositivos, existem algumas restrições associadas a estes: consumo energético, implementação, custos de manutenção e potencial para uma solução de grande escala, tendo em conta o aumento constante de dispositivos da rede, são algumas das preocupações que são consideradas aquando o dimensionamento de uma rede IoT. É com o intuito de intervir nestes tópicos que surgiram as *Low Power Wide Area Networks (LPWANs)*. Veiculada pelo conceito de *Smart City*, as LPWANs são vistas como uma tecnologia que viabiliza a recolha de informação em cenários reais em diferentes tipo de escala, nomeadamente em cenários com grandes áreas.

Long-Range (LoRa), uma das LPWANs disponíveis no sector, enfatizam a comunicação a longa distância com a capacidade de obter sensibilidades de recepção altas, o que permite que estas ligações consigam operar abaixo da interferência causada pelo ruído. Utiliza uma técnica de modulação derivada da *chirp spread spectrum (CSS)*, fazendo com que seja a melhor solução para soluções de IoT que requerem comunicação a longas distâncias, enquanto mantém o consumo energético no mínimo possível. Por outras palavras, a taxa de penetração de sinais LoRa faz com que seja possível estabelecer cobertura suficiente mesmo em cenários de difícil alcance, tais como dispositivos localizados em *indoor*.

Contudo, os métodos usados para aferição da qualidade e fiabilidade dos diferentes tipos de cenários impostos pela realidade, provam ser exigentes e por vezes quase impossíveis de replicar. Esta necessidade motivou o desenvolvimento de simuladores para diferentes tipos de redes de IoT.

Existem múltiplos simuladores de LoRa utilizados pela comunidade científica (como por exemplo: módulo de LoRaWAN para o ns-3, FLoRa e o LoRaSim) cada um com as suas própias aplicações e limitações. O LoRaSim foi o simulador escolhido como base de desenvolvimento nesta dissertação, devido às suas funcionalidades de rede e facilidade em aceder ao seu código fonte para continuar o seu desenvolvimento.

Esta dissertação aborda o desenvolvimento de um simulador para redes LoRa, estudando o impacto que os modelos de propagação e de captura têm em redes deste tipo. Este simulador utiliza alguns dos desenvolvimentos feitos no LoRaSim, mas distingue-se pela capacidade de configurar a rede com maior detalhe, permitindo a utilização de diferentes parâmetros - *Spreading Factor (SF), Bandwidth (BW), Code Rate (CR)* e *payload* - nos dispositivos que compõem a rede, além da inclusão de um módulo externo de planeamento de rede. São realizadas análises a diferentes tipos de redes (pequena/larga-escala, uma/várias *gateways*) de forma a compreender como é que a escolha de dispositivos e de localização da(s) *gateway(s)* influência a qualidade da rede.

Inicialmente, surgiu a necessidade de utilizar um novo modelo de propagação, devido ao curto alcance que o cálculo empírico no modelo de propagação log-distance utilizado pelo LoRaSim tinha. Isto levou à consideração de um novo modelo de propagação a ser utilizado pelo simulador, sendo Okmura-Hata o escolhido. Este modelo de propagação foi escolhido devido à sua popularidade e eficiência em sistemas rádio aplicados a cenários urbanos, que é um dos focos desta dissertação aquando a análise do potêncial do simulador aplicado a simulações de *smart cities*. Os resultados evidenciam que, quando comparado com o modelo de propagação utilizado originalmente, o modelo de propagação de Okumura-Hata dispõe de uma cobertura superior, levando a uma capacidade também superior em relação ao número total de dispositivos suportado pela rede, assim como a possibilidade de maior flexibilidade no posicionamento dos dispositivos, uma vez que a cobertura subiu de 100 metros para 4 quilómetros.

Outro foco de atenção nos desenvolvimentos foi o efeito de captura. Desta forma, foi implementada uma alternativa ao modelo de gestão das colisões na rede. A natureza destructiva do protocolo pure-ALOHA e o efeito de captura mais utilizado, de 6 dB, provam ser abordagens pessimistas e irrealistas aquando o estudo de redes LoRa, levando a redes com prestações aquém do esperado, especialmente quando se analisam redes de grande escala. Por estas razões, o efeito de captura não destructivo foi

implementado. Esta abordagem demonstrou um ganho significativo na qualidade da rede (mais de 20% no pior dos cenários), o que se traduz em redes com melhor desempenho face às outras duas opções. Os resultados de vários ensaios demonstram que a utilização deste método como efeito de captura é relevante independentemente do tamanho da rede, mostrando prestações superiores especialmente em cenários densamente populados, onde a diferença entre os três modos favorece o efeito de captura não destructivo.

Utilizando os desenvolvimentos efectuados no simulador, foram feitas simulações de diferentes cenários de *smart cities*, variando os parâmetros dos dispositivos e o número destes na rede. Os resultados demonstram que existe um limite para a quantidade de *gateways* que conseguem beneficiar a rede, porque em cenários de grandes densidades de dispositivos com as mesmas características, a rede já se encontra saturada, e o custo de implementação de novas *gateways* não compensa o aumento do desempenho obtido com a adição destas. Este fenómeno é mais notável em áreas onde os dispositivos funcionam com *data rates* mais rápidos, promovendo o número de colisões devido ao seu alto débito e falta de ortogonalidade partilhada entre estes.

Os resultados obtidos mostram que os modelos (de propagação e de captura) assumidos no LoRaSim são demasiado simplistas, levando a resultados que ficam aquém do esperado em cenários reais. Quando é utilizado um modelo de propagação orientado a ambientes urbanos (Okumura-Hata) juntamente com um modelo de captura mais realista numa rede que fomenta a heterogeniedade ao usar dispositivos com caracteristicas diversas, o simulador torna-se mais realista e consequentemente - uma vez que os modelos utilizados não eram os adequados e eram demasiado pessimistas - a qualidade da rede aumenta significativamente.

Como trabalho futuro, são propostos alguns desenvolvimentos que levam à melhoria de algumas características já existentes e implementações de novas funcionalidades. A inclusão de antenas directivas como opção em cenários onde não é possível colocar uma *gateway* para server os dispositivos dessa zona é uma das ideias de implementação futuras. Adicionalmente, a opção de poder calcular dinamicamente qual o tempo médio entre mensagens de dispositivos baseado nos parâmetros escolhidos, dando a opção ao utilizador de escolher, além das opções que são possíveis actualmente, qual o *duty cycle* a usar pela rede. Outra implementação pertinente para o simulador seria a inclusão de um módulo adicional a desempenhar a função do *network server*, que iria optimizar ainda mais a rede ao utilizar a função de *Adaptive Data Rate (ADR)* para ajustar dinâmicamente os parâmetros dos dispositivos com base na distância a que estes se encontram da *gateway*, além de filtrar todos os pacotes duplicados que são gerados pelo standard da comunicação em LoRa.

O trabalho desenvolvido no âmbito desta dissertação contribuiu para a melhoria e desenvolvimento de novas funcionalidades, que resultaram num novo simulador que utiliza algumas das funções implementadas pelos criadores do LoRaSim, relacionando o modelo de propagação de Okumura-Hata, um modelo mais optimista como efeito de captura (não destructivo) e uma maior liberdade da parte do utilizador para configurar uma rede LoRa.

Palavras-chave: Redes LoRa, planeamento de rede, modelo de propagação, efeito de captura, avaliação de desempenho

Contents

List of Figures

List of Tables

Acronyms

3GPP	3rd Generation Partnership Project. 11, 25
ADR	Adaptive Data Rate. 20, 21, 40, 44, 86
bps	bits per second. 7
BPSK	Binary Phase-Shift Keying. 13
BW	Bandwidth. 4, 17, 31, 33, 34, 39, 54
CCA	Clear Channel Assessment. 27
CF	Carrier Frequency. 4, 18, 35
CloudRAN	Cloud Based Radio Access Network. 13
CR	Code Rate. 4, 18, 33, 34, 39, 52, 54
CRC	Cyclic Redundancy Check. 19
CSMA	Carrier-Sense Multiple Access. 26, 27
CSS	Chirp Spread Spectrum. 16
DBN	Distance Between Nodes. 32
D-OFDM	Distributed Orthogonal Frequency Division Multiplexing. 16
DBPSK	Differential Binary Phase-Shift Keying. 14
DER	Data Extraction Rate. 4, 44, 45, 46, 47, 48, 53, 59, 63, 66, 67, 70, 71, 72, 75, 76, 78, 79, 80, 81, 82, 84, 86
DR	Data Rate. 20, 29, 33, 39, 57, 58, 59, 67, 71, 78, 84
DSSS	Direct Sequence Spread Spectrum. 14
eMTC	enhanced Machine Type Communications. 8
FDMA	Frequency Division Multiple Access. 14
FEC	Forward Error Correction. 17, 19
FER	Frame Error Rate. 37, 38
GMSK	Gaussian Minimum Shift Keying. 14

GPRS General Packet Radio Service. 12
GSM Global System for Mobile. 12
IoT Internet of Things. 1, 27, 28
ISM Industrial, Scientific and Medical. 9, 30
LoRa Long-Range. 2, 3, 4, 5, 7, 17, 18, 22, 23, 26, 27, 40, 55, 57, 85
LoRaWAN Long Range Wide Area Network. 3, 20, 22, 26, 27, 28, 31, 39
LPWAN Low-Power Wide Area Network. 2, 5, 7, 25, 27, 28
LTE Long Term Evolution. 11
LTE-MTC Long Term Evolution - Machine Type Communications. 8
M2M Machine-To-Machine. 7
MAC Medium Access Control. 3, 20
Mbps mega bits per second. 7
MCL Maximum Coupling Loss. 30, 33, 54
MND Maximum Node Distance. 31, 32
NB-IoT Narrowband-IoT. 8
ND Node Distance. 33
NEC Network Energy Consumption. 38, 39
NF Noise Figure. 31
NFC Near Field Communication. 15
NLOS Non-line-of-sight. 25
ns-3 Network Simulator 3rd Generation. 27
OFDM Orthogonal Frequency Division Multiplexing. 12, 16
OH Okumura-Hata. 4, 25, 29, 30, 40, 41, 51, 54
ppm parts per million. 18
PRB Physical Resource Block. 12
QAM Quadrature Amplitude Modulation. 14
QPSK Quadrature Phase Shift Keying. 14
RAN Radio Access Network. 13
RF Radio Frequency. 20, 85
RPMA Random Phase Multiple Access. 14
RSSI Received Signal Strength Indication. 34, 36, 37, 38, 40, 41, 48, 53, 58, 61, 86
SC-FDMA Single Carrier Frequency-Division Multiple Access. 12
SF Spreading Factor. 4, 18, 31, 33, 34, 35, 39, 54
SNOW Sensor Network Over White Space. 16
SNR Signal to Noise Ratio. 18, 31

TCXO Temperature Compensated Crystal Oscillator. 18
TDMA Time Division Multiple Access. 14
Telensa's PLANet Public Lighting Active Network. 15
TOA Time on Air. 21
TP Transmission Power. 4, 17, 39
UNB Ultra-Narrow Band. 10
Weightless SIG Weightless Special Interest Group. 14
WSN Wireless Sensor Network. 27

Glossary

R_c Chip Rate . 17
d Distance . 30, 31, 33
f_c Carrier Frequency . 30
h_b Gateway Height . 30
h_m Node Height . 30
P_{rx} Receiving Power . 33, 54
P_{tx} Transmission Power . 30, 39
S Sensibility . 30

1

Introduction

This section provides the purpose and motivations that led to the work developed in this dissertation and its consequent writing. Section 1.1 presents the background context for this dissertation. Section 1.2 offer some topics that motivate the work done in this document. Section 1.3 presents the objectives achieved by this dissertation. Section 1.4 shows the contributions offered by the development of this dissertation and section 1.5 details the document's organization.

1.1 Context

Nowadays the need for information is rapidly increasing, urging the development of technology to achieve methods to obtain reliable information. This is possible with the concept of wireless communications and the Internet of Things (IoT).

The IoT, for the last years, has been seen as a technology with a great potential to address many challenges faced by the society: energy resources optimization, air pollution monitoring and climate change prediction are some of the issues that IoT can help. According to a forecast conducted by International Data Corporation (IDC), 30 billion connected (autonomous) things are predicted to be part of the IoT by 2020 [1]. These devices have many areas of applications, for instance: communications, energy, transportation, healthcare to name a few (Figure 1.1). Whatever the use for this technology, there are some constraints attached to it: energy consumption, deployment, maintenance costs and potential of a large scale solution given the continuously increasing

number of devices, are some of the concerns that are factored when dimensioning a IoT network.

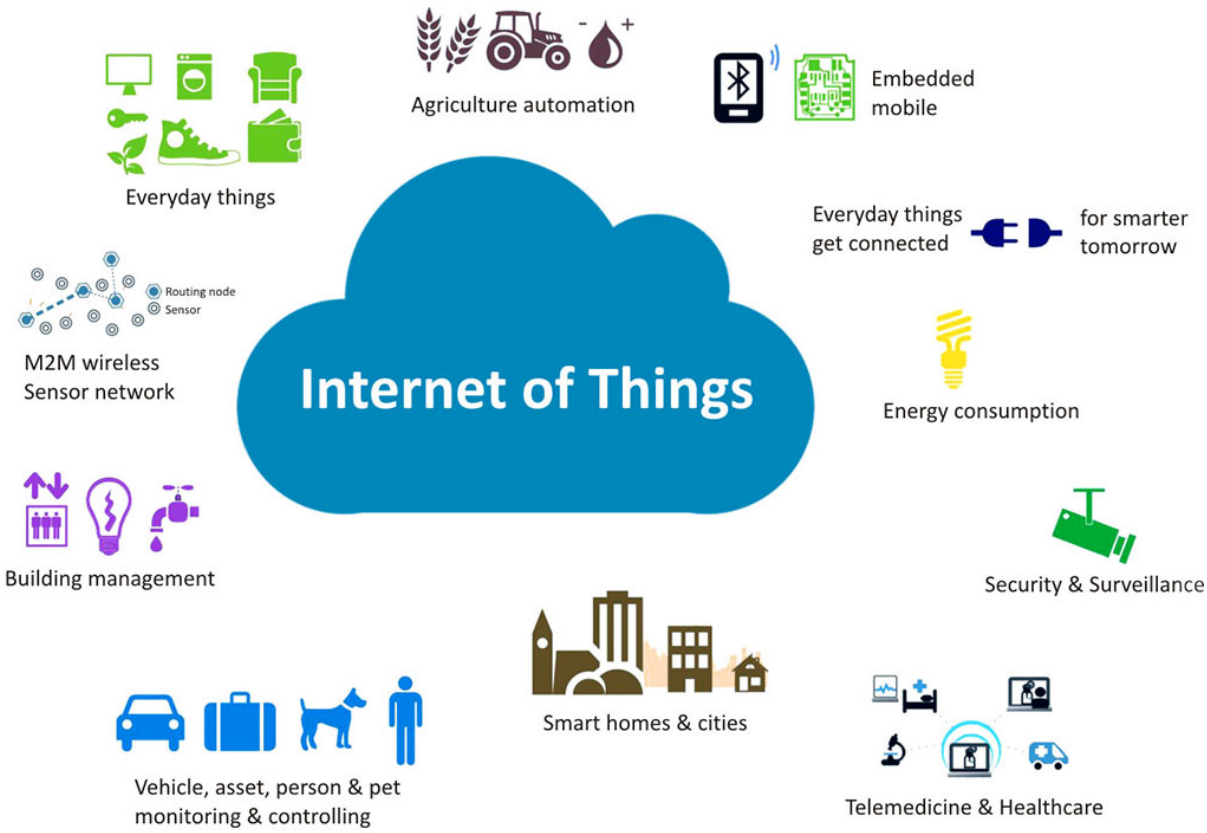

Figure 1.1: Internet of Things applications [2].

To help address these topics, Low-Power Wide Area Networks (LPWANs) have emerged to help enable wireless communications over long distances. LPWANs can achieve this by making the IoT devices send small packets of information with a certain periodicity, by external triggers or even at a programmed interval by the device user. These characteristics allow a system to be efficient, forcing the devices - which are battery-powered and are needed to last for many years - to send small amounts of data periodically over large distances at times.

Long-Range (LoRa), one of the LPWANs available on the market, emphasizes on the long-range communication with the high receiving sensitivity ability which allows it to work under the noise interference or noise floor effectively. It uses a spread spectrum modulation technique derived from chirp spread spectrum (CSS) technologies [3], making it the best option for IoT solutions which required a long range of data

communication while keeping very little power usage. In other words, the strong penetration of the LoRa signal makes it able to provide enough coverage, even in difficult-to-reach scenarios, such as devices located in deeply indoor points [4].

1.2 Motivation

The use of the LoRa technology is the core of this dissertation, using the Long Range Wide Area Network (LoRaWAN) as the adopted Medium Access Control (MAC) to study the impact of a large-scale network and the performance of its devices, using a LoRa simulator.

There are multiple LoRa simulators known to the scientific community, such as the LoRaWAN module for the ns-3 [5], the FLoRa [6] and the LoRaSim [7], each with their own applications and limitations. The LoRaSim was the simulator picked to use in this dissertation, due to the network functionalities it has and the easiness to access it source code to continue further development.

This simulator had different shortcomings regarding network simulation, not allowing to replicate what resembles a real scenario when simulating LoRa networks (i.e. it uses a propagation model that only fitted the simulator authors, a more conservative capture effect and the impossibility to tweak the network into more detail)

The motivation to develop a new simulator emerged from this limitations, with the goal to create a simulator that would enable more customization when planning small or large scale LoRa networks.

1.3 Objectives

The goal of this dissertation is to develop a software simulator to be able to emulate IoT networks, using the LoRaWAN protocol. This simulator was developed taking into consideration some network characteristics developed by the LoRaSim developers, taking it further with additional perks in the new developed simulator.

Since LoRaSim only performs an high level analysis to the network (i.e. it is only possible to see results concerning the network as a whole, without diving into the detail of each device), the interest of having the possibility to tweak the devices in more depth arose, leading to the development of a new simulator.

The objectives of this dissertation are the following:

- Development of functionalities to enable the capacity to perform a network analysis (i.e. number of packets sent, number of collisions, number of received packets and Data Extraction Rate (DER) at a more detailed level (by group of devices);
- Implementation of the Okumura-Hata (OH) propagation model and result comparison with the default empiric propagation model used on LoRaSim;
- Study and integration of the non-destructive capture effect as an alternative to the more conservative 6 dB method;
- Dimensioning of IoT devices with multiple transmission parameters, based on the parameter settings of each device group: Transmission Power (TP), Carrier Frequency (CF), Spreading Factor (SF), Bandwidth (BW) and Code Rate (CR);
- Implementation of dynamic packet size transmission;
- Inclusion of multiple gateways in the same network and corresponding analysis;
- Development of a network planner module.

1.4 Contributions

This dissertation has accomplished the following:

- Enhancement and additional development of a LoRa simulator using the LoRaSim as a foundation [7];
- Insights on how the choice of the propagation model influences the network coverage;
- Performance analysis of a large scale IoT network using the Okumura-Hata propagation model;
- Performance analysis of the destructive mode, 6 dB and non-destructive capture-effect in different types of LoRa networks;
- Performance analysis of multiple gateway use in LoRa networks.

Part of the work presented in this dissertation, namely the LoRa simulator development presented on chapter 3, resulted in a scientific paper submitted and accepted to be presented at the 2021 Telecoms Conference (ConfTELE) [8].

1.5 Document Organization

The remaining document is organized as follows:

- **Chapter 2** discusses the state of the art about LPWANs, reviewing the different types of technologies. At the end of this chapter some relevant related work is presented, mainly regarding the performance of LoRa with different deployments;
- **Chapter 3** presents the enhancements and developments of the LoRa simulator;
- **Chapter 4** shows the performance of the simulations in a more realistic approach to a LoRa network in different type of networks, mixing multiple scenarios;
- **Chapter 5** concludes the dissertation, discussing the results and pointing the direction for future work.

2

State of the art

2.1 Introduction

This chapter focuses on providing the reader content that can serve as knowledge to understand this dissertation, as well as existing work developed by others. Section 2.2 covers the LPWAN subject, showcasing the characteristics of such networks and their pros and cons, while also going in more depth about the LoRa technology. Section 2.3 overviews the related work about LoRa propagation models, LoRa capture effect and LoRa simulators. Finally, section 2.4 recaps the chapter related topics.

2.2 Low-Power Wide Area Networks

The IoT concept is strongly tied with the objective of allowing any object to be connected with the Internet, with data links varying from few bits per second (bps) to mega bits per second (Mbps) and distances varying from less than a meter to multiple kilometers [9]. This landscape is considered to have a great impact on communication service providers, since there is the potential of having a deployment of devices where humans already inhabit [10].

LPWANs are a must have for an expansion of large scale networks, since it provides connectivity to devices (sensors, controllers, Machine-To-Machine (M2M) communications) placed virtually anywhere, offering a long range connection, extended

battery life for the devices and at a low cost, thus providing remarkable advantages.

In the same way there is a wide array of possibilities as applications for IoT (wireless sensor networks, advanced infrastructure for smart metering such as electricity or water, and smart cities), this is also true for the LPWAN solutions that are available to take into consideration. Some solutions available in the market are: LoRa [11], Wi-SUN [12], Sigfox [13], RPMA [14], Weightless [15], DASH-7 [16] and NB-IoT [17]. The most popular technologies operating under unlicensed frequencies are Sigfox and LoRa. Operating under licenced frequency bands are enhanced Machine Type Communications (eMTC) (which belongs to Long Term Evolution - Machine Type Communications (LTE-MTC)) and Narrowband-IoT (NB-IoT).

The LPWAN technologies aimed to connect an impressive number of end-devices (Figure 2.1) by providing them with very low prices where the subscription fee per device is only 1$, thus making them very popular and even rivalling other short-range wireless technologies [18].

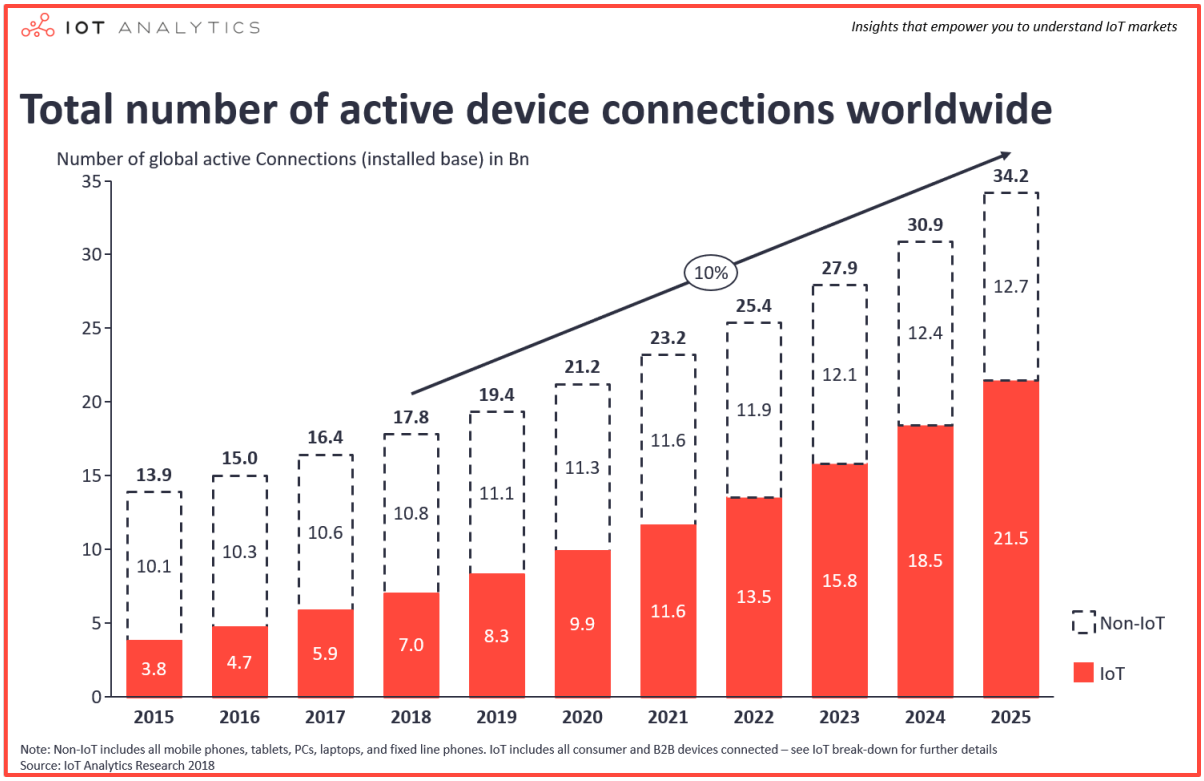

Figure 2.1: Number of connected IoT devices over the years [19].

Due to the typical star network topology, in which the end-nodes (devices) are connected directly to a sink (gateway/base station), there is a high flexibility of device implementation an mobility to some extent [20]. This combined to the fact that these

technologies can operate under unlicensed bands (e.g. Industrial, Scientific and Medical (ISM) band) even knowing the constraints of interference from other devices, make it a valid, if not the best at the moment, solution for an IoT network [21].

2.2.1 Characteristics

Some of the LPWANs characteristics are shared with other wireless technologies. However, unlike wireless technologies that emphasize higher data rate, lower latency and a higher reliability, LPWAN key factors are long range connections with low power consumption and at a low cost (Figure 2.2).

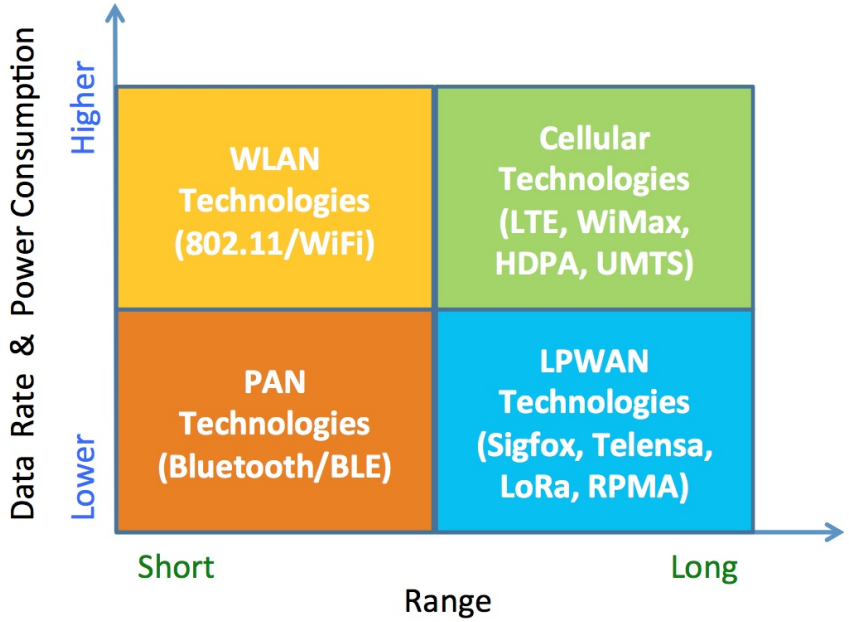

Figure 2.2: LPWAN characteristics compared to other wireless technologies [22].

The main characteristics of LPWAN technologies are [23, 24]:

- **Long range of communications:** The majority of the LPWAN technologies operate on low frequencies (sub-GHz band), which in turn provide for long communications range, varying based on the environment (urban versus rural). Since lower frequencies have better propagation characteristics through obstacles, this makes the sub-GHz band a good candidate, even more having unlicensed bands with these frequencies at disposal;
- **Low power consumption:** IoT devices are expected to last for a long period of time (10+ years) without the need for battery replacement. This is achieved by the use of the star topology, which eliminates the energy consumed through packet

routing in multi-hop networks. Another strong characteristic is keeping the devices simple, by delegating the complexity of the network to the gateway. At last, LPWANs use narrowband channels, decreasing the noise-level and extending the transmission range;

- **Reliability and Robustness:** LPWANs are designed to provide reliable and robust communications. To increase the signal resistance to interference and to provide a certain level of security, most LPWANs adopt robust modulation techniques and spread-spectrum;

- **Low cost of device and deployment:** This is a factor that highly contributed to the success of LPWANs. Non-cellular LPWANs require little to no infrastructure at all, and operate on unlicensed spectrum, providing an excellent alternative to the cellular network. In addition, the advances made in the hardware design and the simplicity of LPWAN end-devices make networks like these economically viable;

- **Full coverage (improved outdoor and indoor penetration coverage):** LPWANs target in enabling better outdoor links and deeper indoor coverage by enhancing the IoT connectivity link budget for 15-20 dB. This is necessary to support devices, such as smart meters, that are located deeply indoor (e.g. in basements, underground parking lots, inside elevators, etc.);

- **Network scalability for the capacity upgrade:** By avoiding multi-hop topology, it has a high potential to scale. Some LPWANs (e.g. LoRa) use multiple antenna systems that allow gateways to support large number of nodes. The scalability of LPWAN is also affected by factors such as the MAC protocol, duty-cycle and reliability requirement.

2.2.2 Technology

There are two options when picking an LPWAN, depending on the type of modulation chosen [25]:

- **Ultra-Narrow Band (UNB):** Using narrowband channels with a bandwidth of the order of 25 kHz. By assigning each carrier a very narrow band, these modulation techniques share the overall spectrum very efficiently between multiple links. The noise level experienced inside a single narrowband is also minimal.

Therefore, no processing gain through frequency de-spreading is required to decode the signal at the receiver, resulting in simple and inexpensive transceiver design. (e.g. Sigfox, Weightless) [26];

- **Wideband:** Using a larger bandwidth (125 kHz or 250 kHz) and employing some form of spread spectrum multiple access techniques to accomodate multiple users in one channel (e.g. LoRa).

Additionally, its possible to chose a technology from two different types: infrastructure based LPWAN (cellular) or infrastructure-less LPWAN (non-cellular) (Figure 2.3). Some of these technologies will be presented, giving more emphasis on the LoRa, since it is the technology in the core of this dissertation.

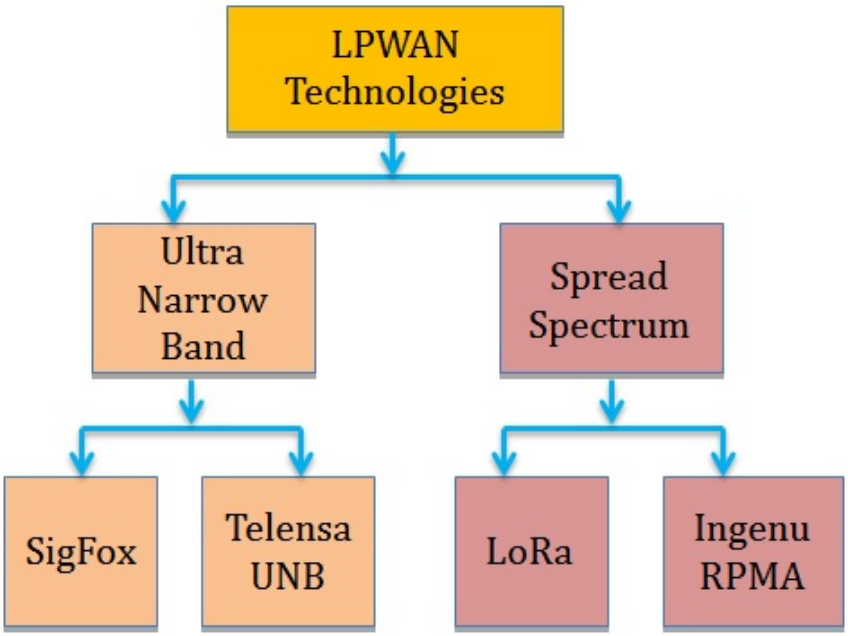

Figure 2.3: LPWAN Technologies for IoT Applications [22].

2.2.2.1 Cellular Technology

NB-IoT is a narrowband LPWAN technology and was developed to be connected using cellular telecommunications band, where it can be shared by Long Term Evolution (LTE) systems. The NB-IoT specification was frozen at release 13 of 3rd Generation Partnership Project (3GPP) specification in june 2016. Further enhancements were made for release 14 and 15, where the latter was frozen in 2018 [27].

It can be deployed in three operation modes - stand-alone as dedicated carrier, in-band within the occupied bandwidth of a wideband LTE carrier, and within the

guard-band of an existing LTE carrier [28]. In stand-alone deployment, NB-IoT can occupy one Global System for Mobile (GSM) channel (200 kHz) while for in-band and guard-band deployment, it will use one Physical Resource Block (PRB) of LTE (180 kHz).

The design targets of NB-IoT include low-cost devices, high coverage (20-dB improvement over General Packet Radio Service (GPRS)), long device battery life (more than 10 years), and massive capacity (greater than 52K devices per channel per cell). Latency is relaxed although a delay budget of 10 seconds is the target for exception reports [29].

In order to support such flexible deployment scenarios, NB-IoT reuses the LTE design extensively, such as Orthogonal Frequency Division Multiplexing (OFDM) in downlink and Single Carrier Frequency-Division Multiple Access (SC-FDMA) in uplink [30].

LTE-M named also LTE CAT-M1 or eMTC, can be deployed on existing LTE networks, fully using current spectrum resources of operators for maximized spectral usage. It is optimized for lower complexity/power, deeper coverage and higher device density, while also coexisting with other LTE services in a seamlessly way [31]. It had a specified coverage enhancement in Rel-13, which provided up to 15 dB of coverage extension, compared to the baseline LTE network [32]. Despite this enhancement, LTE-M coverage is shorter than the NB-IoT, as seen in Figure 2.4

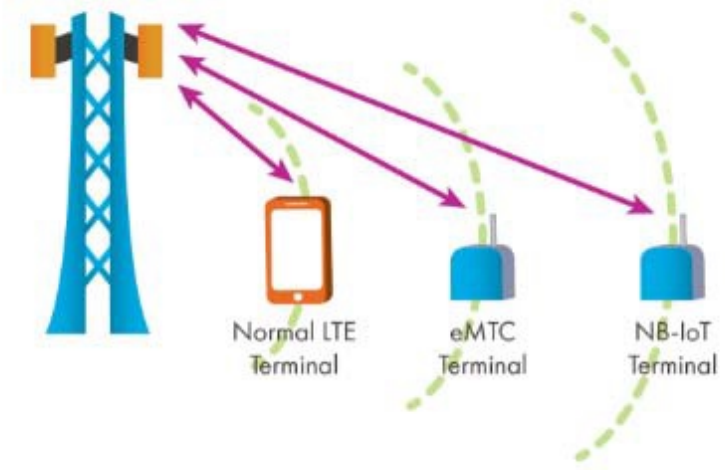

Figure 2.4: LTE-M range [31].

5G-IoT is expected to provide applications with real-time, on demand, which requires the 5G-IoT architecture to be able to deal with end-to-end coordinated, agile,

automatic, and intelligent operations during each phase. Its unique combination of high-speed connectivity, very low latency, and ubiquitous coverage will support smart vehicles and transport infrastructure such as connected cars, trucks, and buses, where a split second delay could mean the difference between a smooth flow of traffic and a 4-way crash at an intersection. The 5G-IoT architectures are expected to provide [33]:

- Logically independent networks according to requirements of applications;
- Use Cloud Based Radio Access Network (CloudRAN) to reconstruct Radio Access Network (RAN) to provide massive connections of multiple standards and implement on-demand deployment of RAN functions required by 5G;
- Simplify core network architecture to implement on-demand configuration of network functions

2.2.2.2 Non-Cellular Technology

SigFox operates under the the ISM unlicensed bands (868MHz in Europe, 915 MHz in North America, and 433 MHz in Asia) [34] and uses UNB modulation. Because of this, the bandwidth is used efficiently and has very low noise levels, low power consumption, high receiver sensitivity and low-cost antenna design. All of this with the expense of having a maximum throughput of 100 bps, which clearly falls at the lower end of the throughput offered by most other LPWAN technologies and thus limits the number of use-cases for Sigfox [26].

The end devices connect to these base stations using Binary Phase-Shift Keying (BPSK) and initiates a transmission by sending three uplink packages in sequence on three random carrier frequencies. The gateway still manages to receive the package even if two messages are lost due to collision or interference from another systems using the same frequency. The duty cycle restrictions of the utilized sub-band in the 868 MHz EU ISM band is 1%. Therefore, a SigFox device may only transmit 36 seconds per hour. The time on air is 6 sec per package and thus the maximum is 6 messages per hour with a payload of 4, 8, or 12 bytes [35]. It is advertised by Sigfox that each gateway can support up to a million connected objects, with a coverage area of 30-50 km in rural areas and 3-10 km in urban areas [25].

INGENU (formerly known as On-Ramp Wireless) proposed a proprietary LPWAN technology compliant to the IEEE 802.15.4k specifications. Unlike most other technologies, it does not rely on better propagation properties of SUB-GHZ band. Instead, it operates in 2.4 GHz ISM band and leverages more relaxed regulations on the spectrum use across different regions [26].

Random Phase Multiple Access (RPMA) was developed based on Direct Sequence Spread Spectrum (DSSS). The data sent is first encoded and then interleaved, resulting in a stream modulated with Differential Binary Phase-Shift Keying (DBPSK). There are some drawbacks concerning propagation when using this band. At 1km distance, Hata [36] modeling shows a typical difference of 15dB in attenuation between 868MHz and 2.4GHz, the latter being also less efficient in penetrating inside buildings [9].

Weightless Special Interest Group (Weightless SIG) is an organization which aims at providing Weightless standards for IoT networks. There are three open LP-WAN standards, each providing different features, range and power consumption. These standards can operate in license-free as well as in licensed spectrum, and are the following [25, 26, 37, 38]:

- **Weightless-W:** Operating with a star topology, this system takes advantage of the TV white space spectrum and provides a wide range of modulation schemes, spreading factors and packet sizes. However, the shared access of the TV white spaces is permitted only in few regions, therefore weightless defines the other two standards in ISM band, which is globally available for shared access;

  The modulations can range vary from 16-Quadrature Amplitude Modulation (QAM) to DPSK in the 470-970 MHz range of the TV band with a wide range of spreading factors (up to 1024).Weightless-W claims to achieve two-way data rates from 1 kbps to 10 Mbps with very low overhead;

  The end devices transmit to base stations in a narrow band but at a lower power level than the base stations to save energy, but due to the extensive feature set provided by Weightless-W, the edge-node's battery lifetime is limited to three years and the terminal cost is higher than that of its competitors. The communication between the edge-nodes and the base station can go up to 5 km (indoor) to 10 km (outdoor);

- **Weightless-P:** Supporting two-way communications, this technology modulates the signals using Gaussian Minimum Shift Keying (GMSK) and Quadrature Phase Shift Keying (QPSK). It supports narrowband channels of 12.5 kHz in ISM band, with Frequency Division Multiple Access (FDMA) and Time Division Multiple Access (TDMA) and adaptative data rates varying from 0.2 Kbps to 100 Kbps. The gateways are time-synchronized to schedule the transmissions in the slots. However, the range is slightly reduced to 2 km in urban environment;

- **Weightless-N:** Using a UNB (DBPSK modulation) in order to provide unidirectional-only connectivity of up to 100 bps (which limits the number of uses cases), by

exploiting ISM bands. This scheme is based on nWave's [39] technology which was donated as a template for the Weightless-N standard. Because of the simplicity of this solution, Weightless-N allows a battery duration of up to 10 years, very low cost terminals, and a long connection range (5 kms even in challenging urban environments) similar to that reached by Weightless-W.

On table 2.1 it is possible to see a breakdown of the three standards.

Standard	**Weightless - W**	**Weightless - N**	**Weightless - P**
Modulation	16-QAM, BPSK, QPSK, DBPSK	UNB DBPSK	GMSK
Band	TV white spaces/470-790 MHz	ISM-Sub-GHZ, EU (868 MHz), US (915 MHz)	Sub-GHz ISM/licensed
Data Rate	1 Kbps - 10 Mbps	30 Kbps - 100 Kbps	200 Bps - 100 Kbps
Range	5 Km (Urban)	3 Km (Urban)	2 Km (Urban)
Nr º of channels	16 or 24 channels (Uplink)	Multiple 200 Hz channels	Multiple 12,5 KHz channels
Topology	Star	Star	Star
Packet Size	>= 10 Bytes	<= 20 Bytes	>= 10 Bytes
Authentication and Encryption	AES 128b	AES 128b	AES 128/256b

Table 2.1: Weightless standards characteristics [26, 38].

Telensa [40] a bi-directional UNB technology using the unlicensed spectrum, is used to transmit small amount of data [22]. Its use is mostly targeted towards the smart cities market, having the Public Lighting Active Network (Telensa's PLANet) for street lightning control and PARKet for smart parking enhancement. Telensa claims range varying from 2-3 km in urban, and 5-8 km in rural environments. This type of solutions are already implemented in different big cities worldwide [38].

Dash7 is an open standard for the license-free (433 MHz and 868/915 MHz) ISM band air-interface for wireless communications promoted by the Dash7 Alliance [16]. By using a two-hops tree topology with hierarchized devices (endpoints, sub-controllers and gateways), offering low-latency with multi-year battery life and a range up to 2km, this network is suitable for direct device-to-device communications and Near Field Communication (NFC) with radio devices. Defined by the BLAST acronym, this network's features are [38, 41]:

Bursty: Transmits short and sporadic sequences of data;

Light: Small packet size limited to 256 bytes;

Asynchronous: Communication is command response based, no periodic synchronization;

Stealth: End-devices communicates with pre-approved gateway. No need for periodic discovery beacons;

Transitive: Supports mobility. End-devices can move seamlessly between different Gateway coverages.

Sensor Network Over White Space (SNOW) is a network that takes advantage over TV white spaces, which refer to the allocated but unused TV channels [42]. One advantage over ISM band bound networks, is the fact that white spaces are less crowded and have an overall wider availability in both urban and specially in rural areas, allowing it to be a good candidate to many applications such as habitat, environment and volcano areas.

Using a star network topology, each sensor node is equipped with a single half-duplex narrow-band white space radio. The nodes are directly connected to the gateway and vice versa [23]. The gateway uses a wide channel split into orthogonal subcarriers, each of equal bandwidth. The PHY layer of SNOW uses Distributed implementation of OFDM for multi-user access, called Distributed Orthogonal Frequency Division Multiplexing (D-OFDM).

2.2.3 Long-Range (LoRa)

Developed by Semtech Corporation [43], LoRa is a wireless technology focused on delivering long range coverage, low power consumption that enable the devices batteries to last for a long time, high network capacity, robust communication and localization capability [44].

LoRa can be divided into two layers: the physical layer, which is property of Semtech, and the MAC layer, which is open and anyone can deploy LoRa stations or networks to offer services as long as the spectrum regulations are respected [45]. Although, the most popular standard for MAC layer is LoRaWAN, which is implemented by the LoRa alliance. Figure 2.5 shows the different layers of the LoRa technology.

2.2.3.1 Physical Layer

LoRa's physical layer radio modulation is based on the Chirp Spread Spectrum (CSS) technique operating in a non-licensed band in the sub-GHz range (EU: 868 MHz and 433 MHz, USA: 915 MHz and 433 MHz) using orthogonal spreading factors, which

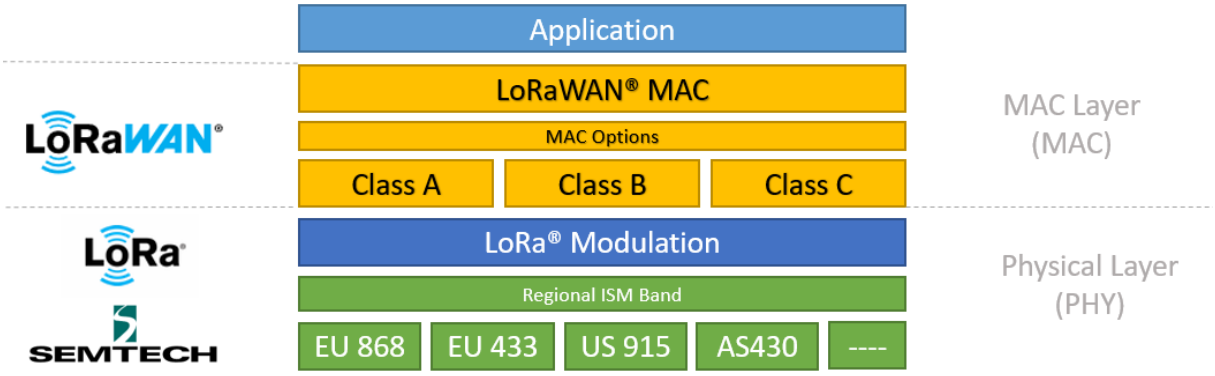

Figure 2.5: LoRa stack [46].

allows the trade of data rate for sensitivity within a fixed channel bandwidth. The relationship between the chirp rate and symbol rate in the LoRa modulation technique is defined in (2.1) where the R_c is equal to the system BW, which stands for the modulation bandwidth (Hz). This technique was developed during the 1940s decade, and was traditionally used in military applications because of its characteristics [47]: long range communications (it is possible to decode transmissions at 19.5 dB below the noise floor), multi-path resistance, robustness, low power consumption, Forward Error Correction (FEC), and Doppler resistance [48].

$$Rs_{[symbol/s]} = \frac{R_c}{2^{SF}} \tag{2.1}$$

There are five parameters that can be adjusted independently in a LoRa network that allow to adjust the transmission range, power consumption and resilience to noise. Those parameters are [49, 50]:

- **Transmission Power (TP):** On LoRa this parameter can be set between -4 dBm and 20 dBm in 1 dB steps. However, due to hardware limitations, the range is often limited to a range of 2dBm to 20 dBm. The chosen sub-band in the operating region and the ISM band dictate a limit to the range of the used power. In this case, on the 868MHz sub-band operating in Europe, the limit is set to 14 dBm. A bigger TP increases the energy consumption, transmission duration (becomes faster), resilience, robustness and range (more wider). Because of hardware limitations, power levels higher than 17 dBm can only be used on a 1% duty cycle;
- **Bandwidth (BW):** range of frequencies in the transmission band. The higher the BW, the better the data rate is (and consequently the shorter the time on air), but

has the trade-off of offering a lower sensitivity (because of integration of additional noise). Lower BW requires more accurate crystals (less parts per million (ppm)). Data is sent at a chirp rate equal to the bandwidth. So, a bandwidth of 125 KHz corresponds to a chirp rate of 125 Kcps. Although the bandwidth can be selected in a range of 7.8 kHz to 500 kHz, a typical LoRa network operates at either 500 kHz, 250 kHz or 125 kHz. Also, bandwidths lower than 62.5 kHz require a Temperature Compensated Crystal Oscillator (TCXO);

- **Spreading Factor (SF):** This parameter represents the ratio between the symbol rate and chip rate. A higher spreading factor increases the Signal to Noise Ratio (SNR), which translates to the increase of sensitivity and range, with the drawback of increasing the air time of the packet. The number of chips per symbol is calculated as 2^{SF}. For example, with an SF of 12 (SF12) 4096 chips/symbol are used. Each increase in SF halves the transmission rate and, hence, doubles transmission duration, and ultimately, the energy consumption. Spreading factor can be selected from 6 to 12. SF6, with the highest rate transmission, is a special case and requires special operations. For example, implicit headers are required. Radio communications with different SF are orthogonal to each other and network separation using different SF is possible;

- **Code Rate (CR):** FEC rate used by the LoRa modem and offers protection against bursts of interference, and it can be set to different modes, such as $4/5$, $4/6$, $4/7$ or $4/8$. A higher CR offers more protection, but increases time on air. Devices having different CR while having the same CF/SF/BW, can still communicate with each other if they use an explicit header, as the CR of the payload is stored in the header of the packet, which is always encoded at $4/8$;

- **Carrier Frequency (CF):** frequency used for the transmission band, which can be programmed in steps of 61 Hz between 137 MHz to 1020 MHz (this is the case for the SX1272 RF transceiver from Semtech). Depending on the LoRa chip that is used, this range may be limited in a range varying from 860 MHz to 1020 MHz.

When two LoRa transmissions overlap at the receiver, there are several conditions which determine whether the receiver can decode, one, two packets, or nothing at all. This depends on the CF and SF parameters, as well the power and timing of the transmission. When this happens, there is the possibility to have the capture effect in play. The capture effect occurs when two signals are present at the receiver and the weaker signal is suppressed by the stronger signal. The difference in received signal strength can therefore be relatively small. When the difference is too small, however,

the receiver keeps switching between the two signals, effectively not able to decode either transmission [50].

The maximum packet size for a LoRa message is 256 bytes, as shown on figure 2.6

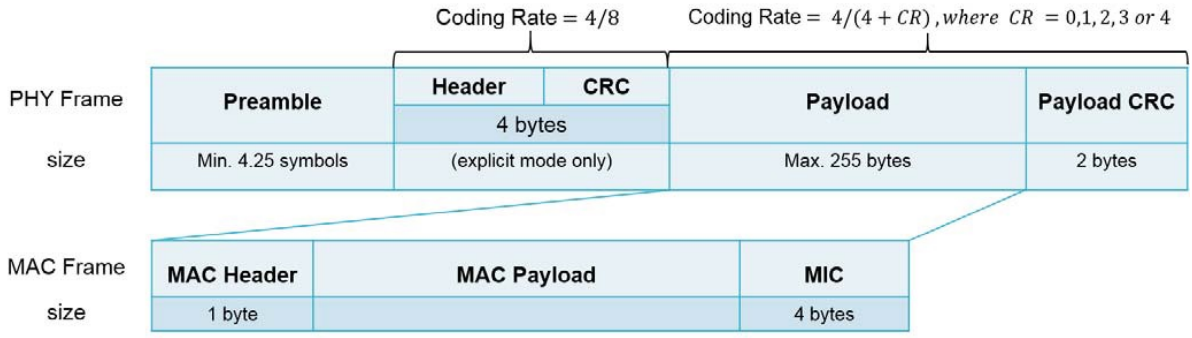

Figure 2.6: LoRa packet structure [51].

The structure of the packet is the following [51]:

- **Preamble field:** Used for the synchronization purposes. The receiver synchronized with the incoming data flow;
- **Header field:** Depends on the choice of two available operation modes. In default explicit operational mode, the number of bytes in the header field specifies the FEC code rate, payload length and presence of Cyclic Redundancy Check (CRC) in the frame. The second implicit operational mode specifies that coding rate and payload in a frame are fixed. In this mode, frame does not contain this field, which gives reduction in transmission time. Header field also contains 2 byte CRC field which allows the receiver to discard packets with an invalid header. Header field along with its CRC field are 4 bytes long and are encoded with 1/2 coding rate, while coding rate for the rest of the frame specifies in PHY header. The first byte of header field specifies the payload length;
- **Payload field:** Maximum payload varies from 2 to 255 bytes. This field further contains following fields:

  MAC header: Defines the frame type (data or acknowledgment), protocol version and its direction (uplink or downlink);

  MAC payload: Contains actual data;

  MIC: Used as the digital signature of the payload.
- **CRC:** Optional field that comprises CRC bytes for error protection for payload (2 bytes).

2.2.3.2 MAC Layer (LoRaWAN)

Developed and maintained by the LoRa Alliance, the LoRaWAN is the MAC layer protocol typically used in LoRa systems solutions. It is optimized for battery-powered end-devices that may be either mobile or mounted at a fixed location.

Supporting a star topology, the communication between the devices and gateways is spread out on different frequency channels, and data rates are determined according to communication range and message duration. This selection can be managed by a LoRaWAN network infrastructure, which selects the data rate and channel for each device using an Adaptive Data Rate (ADR) scheme [41]. The LoRaWAN has been chosen as the LPWAN solution in both regional and urban areas [52], having gateways designed for outdoor or indoor use, while also enabling the use for public and private network deployments [53].

A LoRaWAN network (Figure 2.7) mainly consists of the following three components [25, 41, 54]:

- **End-Device:** Sensors, detectors or actuators connected via the LoRa radio interface to one or more LoRa Gateways via single-hop communication;
- **Gateway:** Concentrators that are responsible to relay messages between end-devices and the Network Server. All the gateways that successfully decode the message sent by an end-device will forward the packet to the Network Server by adding some information regarding the quality of the reception;
- **Network Server:** The most sophisticated hardware piece of the network. The Network Server controls the whole network (radio resource management, admission control, security, etc) and is responsible for detecting duplicate packets, choosing the appropriate gateway for sending a reply (if any), consequently for sending back packets to the end-devices. A distinguishing feature of the LoRaWAN is the ADR, which allows the Network Server to adapt the transmit rate of an end-device by changing the SF index, in order to find the best trade-off between energy efficiency and link robustness.

The ADR allows for a power-saving mechanism, adjusting the data rate and the Radio Frequency (RF) output power according to the distance of the node from the gateway. This method is flexible enough to accommodate changes in the network infrastructure and support varying path loss. Data Rate (DR), calculated with equation (2.2), can vary depending on the application [55].

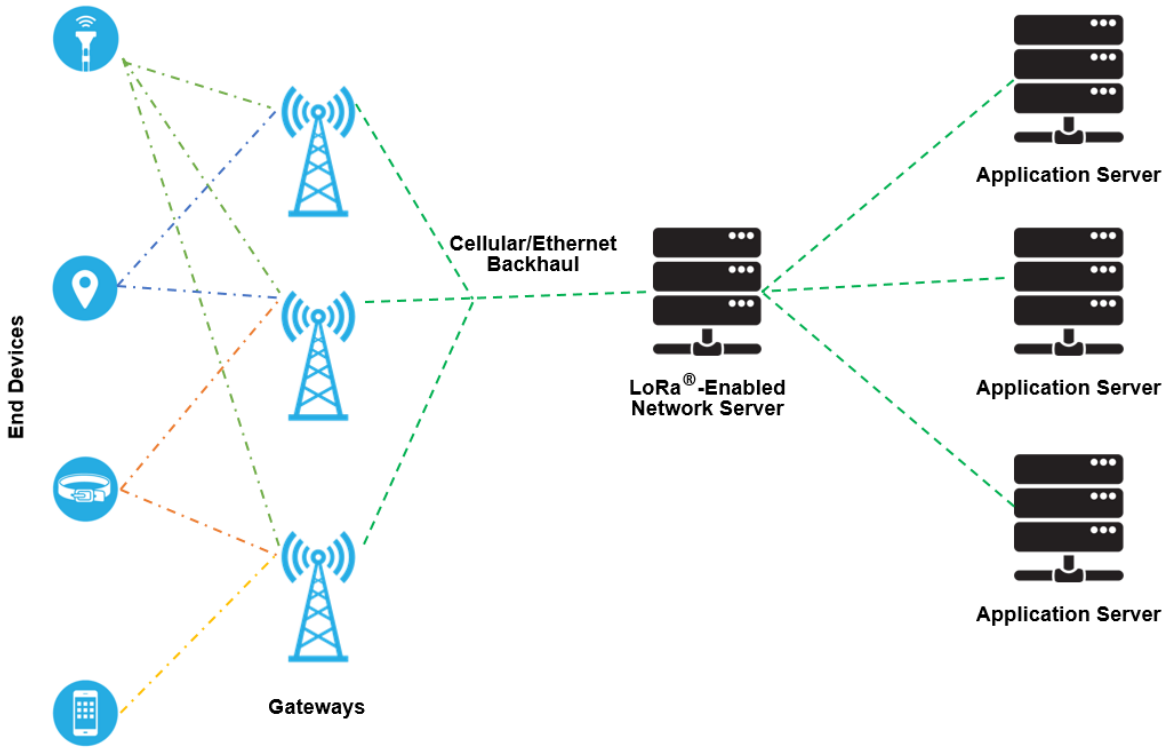

Figure 2.7: LoRa Network [55].

Generally speaking, the ADR technique tries to use the highest possible data rate at all times (therefore, reducing the Time on Air (TOA) of a packet and the energy needed to transmit the same packet). However, there is also a caveat to this: by increasing the data rate, the chance that a transmission not being received due to interference also increases [56].

$$DR_{[bps]} = SF \times \frac{BW_{[kHz]}}{2^{SF}} \times \frac{4}{4+CR} \tag{2.2}$$

On a LoRaWAN network, the end nodes operate asynchronously with the network and use the ALOHA protocol, which means that they are only activated when there is a need to send information. This translates into more battery lifetime, allowing the devices to last for a longer period of time.

These nodes can be divided into three different device classes according to the trade-off between network downlink communication latency versus battery life [9, 25, 38]:

- **Class A (for All):** End-devices of Class A allow for bi-directional communications whereby each end-device's uplink transmission is followed by two short

downlink receive windows. The transmission slot scheduled by the end-device is based on its own communication needs with a small variation based on a random time basis (ALOHA-type of protocol). This class is the lowest power end-device system for applications that only require downlink communication from the server (i.e. monitoring applications, where data produced by the end-devices have to be collected by a control station) shortly after the end-device has sent an uplink transmission. Downlink communications from the server at any other time will have to wait until the next scheduled uplink;

- **Class B (for Beacon):** In addition to class A functionality, devices in this class open extra receive windows at scheduled times. This requires a synchronization beacon for proper operation, which is advertised by the gateway. This class is used by devices that need to receive commands from a remote controller (i.e. switches or actuators, or devices that provide data at user's request);

- **Class C (for Continuously Listening:** End-devices of Class C have almost continuously open receive windows, only closed when transmitting. This class is used for end-devices without (strict) energy constraints (i.e. connected to the power grid). Therefore, this class has the lowest latency and the highest consumed power.

There are two layers of security that are used in this network: one for the network and one for the application. The security at the network level ensures authenticity of the node in the network, while the security at the application layer ensures the network operator does not have access to the end user's application data [9].

It is stated that the LoRaWAN networks should only use available ISM frequency bands. By doing so, the network is impaired by the regulations that these bands have, regarding the maximum transmission power and the duty cycle. These duty cycle limitations translate into delays between the messages sent by the devices [54]. For instance, if we consider the maximum duty cycle for the EU ISM 868 MHz band of 1%, it corresponds to a 36s per hour of up-time in each sub-band, for each end-device (equation (2.3)) [57].

$$Toff_{subband} = \frac{FrameAirTime}{DutyCycle_{subband}} - FrameAirTime \tag{2.3}$$

On table 2.2 there is a showcase comparing the differences with other cellular technologies. As seen, the LoRa has some trade-offs when compared to other cellular technologies, offering competitive results considering its lower cost implementation.

	LoRa	**NB-IoT**	**UNB**	**LTE-M Rel. 12/13**	**LTE-M Rel.13**	**EC-GSM Rel.13**
Range	< 11 km	< 35 km	< 13 km	< 11 km	< 15 km	< 15 km
Max. coupling loss	157 dB	160 dB	164 dB	156 dB	164 dB	164 dB
Spectrum Bandwidth	Unlicensed 900 MHz < 500 kHz	Unlicensed 900 MHz < 100 Hz	Licensed 7 - 900 MHz 200 kHz	Licensed 7 - 900 MHz 1.4 MHz or shared	Licensed 7 - 900 MHz 200 KHz or shared	Licensed 8 - 900 MHz 2.4 MHz or shared
eData rate	10 Kbps	< 100 bps	< 170 Kbps (DL) < 250 Kbps (UL)	< 1 Mbps	< 150 Kbps	< 10 Kbps
Indoor	Yes	No	Yes	No	Yes	Yes
Security	No	No	Yes	Yes	Yes	Yes
Bi-directional	Yes	Yes	Yes	Yes	Yes	Yes
Global ecosystem	No	No	Yes	Yes	Yes	Yes
Battery life	> 10 years	> 10 years	> 10 years	> 10 years	> 10 years	> 10 years

Table 2.2: LoRa vs cellular technologies [24].

Table 2.3 does a comparison with other non-cellular technologies. When taking into consideration all the characteristics present on the table, LoRa offers the highest transmission range combined with mobility, a decent battery lifetime, indoor compatibility and a considerable link budget.

	LoRa	**SigFox**	**RPMA**	**Telensa**	**DASH7**	**SNOW**
Modulation	CSS	DBPSK, GFSK	DSSS, CDMA	FSK	GFSK	BPSK
Band	Unlicensed, Sub-GHz	Unlicensed, Sub-GHz	Unlicensed, 2.4 GHz	Unlicensed, Sub-GHz	Unlicensed, Sub-GHz	Unlicensed, TV white spaces
Max Range (Km)	15	10	15	1 - 10	0 - 5	5
Peak data rate (Kbps)	27	1	80	65	9.6, 55.666, 166.766	50 Kbps per node
Security	Yes	Yes	Yes	Yes	Yes	N/A
Indoor	Yes	No	Yes	No	No	Yes
Link budget (dB)	164	N/A	177	N/A	N/A	N/A
Mobility	Yes	No	Limited	No	N/A	N/A
Battery lifetime (Years)	10	5	15	10	N/A	N/A

Table 2.3: LoRa vs non-cellular technologies [24].

2.3 Related Work

In this section some work related to the topics covered in this dissertation are presented.

2.3.1 LoRa Propagation Models

After showcasing the different LPWANs and their features, it is of general consensus that this technology is very relevant to the IoT paradigm. As such, it is important to discuss the different propagation models that are applied to this type of networks, more specifically LoRa.

Lauridsen et. al [4] conducted tests on urban environments using their own calibrated version of 3GPP Urban Marco Non-line-of-sight (NLOS) model. The area studied was the north Denmark region with 7800 km^2 of rural area, predominantly farm land, forest and smaller villages. There is also a combined urban area of 147 km^2. This study was performed on a already used Telenor network. Results show that even over 30dB additional penetration loss, LoRa has an outage of 0.32% for the urban locations, 24% for rural areas and 20% for urban and rural areas combined.

Zainal et. al [58] studied the use of the log-distance path loss model when developing LoRa networks. It is shown in their research that the shadowing effect plays a considerable role in determining the overall performance of such networks. Environments that are composed by dense foliage have a serious handicap in network coverage, leading to careful planning and consideration when dimensioning a network in these conditions.

Hosseinzadeh et. al [59] performed tests on multi-wall models (COST231 and Motley-Keenan) overall performance. It is shown that these models are considered the best candidates for indoor LoRa scenarios, by retaining an acceptable trade-off between the complexity and accuracy. The attenuation and permittivity factors clarify that the real-world obtainable performance of this LPWAN technology is achieved by the use of classical propagation models.

With the multiple studies presented in this subsection, it is possible to assume that the propagation model plays an important role when analyzing the performance of a LPWAN. In this dissertation the choice of the propagation model takes into consideration the urban environment, and as such, the OH is a propagation model that offers an high range connectivity to a urban network, making it a suited alternative to the work developed in this document.

2.3.2 LoRa Capture Effect

Besides 0 dB method traditionally used by a LoRa network, there are studies of other mechanisms to improve the overall efficiency of these kind of networks. Essentially, the capture effect is the ability to receive one or more of the several packets that collided, when certain conditions apply. Most of the time these researches show that when a capture-effect is used, the amount of packets lost by the gateway is reduced thus making the network better as a whole.

Noreen et. al [60] show that the probability of a successful transmission is enhanced when a capture effect technique is applied to the LoRa network. They concluded that the overlapping length of a packet and the interferer packet signal received power have influence in the capture effect.

Bankov et. al [61] considered a LoRaWAN with 1000 nodes and compared the results between a 0 dB network and their own take at the capture-effect through their mathematical model. Their model says that if the frame's power is greater than the interferer frame power plus thermal noise, the packet is received. Their results show that the collisions drop 50% when compared to the typical ALOHA approach. As a result, the maximum capacity of the network without exceeding the same number of collisions (capture effect vs ALOHA) can be up to 100% higher.

Beltramelli et. al [62] through their stochastic geometry-based model evaluate the performance of the capture effect on pure-ALOHA, slotted-ALOHA and Carrier-Sense Multiple Access (CSMA) LoRa networks. Despite the advantages and disadvantages that each random access protocol offers, the only thing that is common across them its the capture effect impact on the network. Their results expose the significant improvement of the channel throughput at large device densities.

Fernandes et. al [63] proposed a probabilistic packet collision model that estimates the success delivery of two and more LoRa concurrent transmissions based on an exhaustive evaluation of the packet capture effect.

Through the study of the capture effect, it is noticeable that when applied this functionality greatly increased the network quality. As such, the research conducted by Fernandes et. al [63] showed consistent results on their own take at the capture effect, and is the chosen study to use in the simulator developed in this dissertation.

2.3.3 LoRa Simulators

There are multiple solutions in the form of software to simulate a Wireless Sensor Network (WSN). In this section some of the most LoRa simulators used by the community are discussed.

To and Duda [64] used the Network Simulator 3rd Generation (ns-3) LoRa module to simulate the behaviour of the network with a CSMA implementation to enhance the overall data rate. Their findings show that using the CSMA to do a Clear Channel Assessment (CCA) to test of an ongoing transmission on the channel (and only starting the communication after the previous ended) provides energy benefits when considering a network with a large number of nodes (4000+). Regarding the packet delivery rate, it is visible that the amount of received packets have significantly increased when using CSMA instead of ALOHA as a media access

Slabicki et. al [65] developed a software simulator called FLoRa, an open-source framework for end-to-end LoRa simulations using the OMNeT++ event simulator. They analyze the effect of the ADR on the delivery ratio of the network, after showing that the ADR, although effective in increasing the network's data rate, is severely affected by a highly-varying wireless channel. With this in mind, they propose an improved version of the original ADR mechanics to cope with the variable channel conditions. Results show that both the reliability and the efficiency of the network has increased over normal circumstances. They finish the article claiming that the network's data rate can be improved by using a network-aware approach, where the link parameters are configured based on the global knowledge of said network.

Bor et. al [50] developed the simulator LoRaSim based on their practical experimentation. They studied the scalability of LPWANs, more specifically LoRaWAN. Using a log-distance path loss model with their own empirical measurements, they claim that LoRaWAN is not a reliable solution when trying to scale up. They show evidence that using conservative transmission settings with only one gateway in range of a node, in a typical scenario where a network has 64 nodes in a area of about 4 ha, proves to the insufficient for future IoT deployments. Their study also shows that dynamic transmission parameters and/or multiple sinks can enable a good network scaling, although more work is needed to develop protocols and strategies for useful sink deployment.

The choice of the LoRa simulator to use in this dissertation was based on the potential to understand and change/implement new code according to the needs of the intended study. Among the different simulators, the LoRaSim offered the best fit to these requirements and therefore was the chosen simulator to be used.

2.4 Chapter Considerations

In this chapter the main concepts of LPWANs were discussed, its characteristics, the basics of the architecture and operation requirements. It was also pointed the benefits offered by the IoT to society in general. Numerous LPWAN technologies were presented, with emphasis on LoRa physical and MAC layer, due to being the bedrock technology used in this dissertation.

At the end of this chapter, some related work to this dissertation was presented. On the propagation models topic, some of the most used and known path loss models were presented and their results briefly discussed. Regarding the capture effect, it was shown that regardless of the used access protocol approach, the capture effect yielded promising results to the performance of the network, specially when compared to a purely destructive model. Finally, some LoRa simulators used and developed by the scientific community were presented, along with all the conclusions and future development needs that are in order for LoRaWAN networks.

The next chapter delivers insights related to the developed simulator for this dissertation. It shows the improvements made over the original LoraSim and offers some discussion about the obtained results.

3

LoRa Simulator

In this chapter, the characteristics of the simulator that was developed taking the LoraSim as baseline will be presented, as well as some analysis over the differences between both implementations. Section 3.1 delivers a detailed explanation of the simulator architecture. Section 3.2 details the simulation using the developed simulator and discusses the results achieved. Finally, section 3.3 recaps the chapter contributions.

3.1 Architecture

The developed simulator uses some of the functionalities that the LoRaSim already has, changing them to accommodate the new developments and implements some new features. This simulator allows a more detailed breakdown of the network, by allowing the configuration of each group of nodes with a corresponding Data Rate and payload. This simulator takes advantage of the Okumura-Hata propagation model characteristics to simulate a urban scenario, instead of the original log-distance propagation model implemented in LoRaSim. Finally, a new model of the capture-effect is also implemented, using a non-destructive probabilistic model.

In this section the global architecture of the developed simulator is discussed. Each subsection provides a breakdown of the steps taken during the development phase.

3.1.1 Initial Parameters

One of the changes to the original simulator was the adopted propagation model. As told in [50], the original path loss model used to describe the network was the log-distance. This showed some constraints when trying to apply it to an urban network, because the decision to use it was based on empirical measurements made by the authors. Because of this reason, and to help solving this constraint, it was decided to use a propagation model that could be generic enough to be used as an universal solution, regardless of the environment where the network is set up. The chosen propagation model was the OH [36], whose Maximum Coupling Loss (MCL) is represented as follows:

$$MCL_{[dB]} = A + Blog(d), \tag{3.1}$$

where the factors A and B can be derived from (3.2) and (3.3) respectively. The distance d is given in kilometers, and is determined based on the respective MCL.

$$A = 69.55 + 26.16log(f_c) - 13.82log(h_b) - a(h_m) \tag{3.2}$$

$$B = 44.9 - 6.55log(h_b) \tag{3.3}$$

Carrier frequency (f_c) is given in MHz, which in this case is set to the 868 MHz sub-band [66], the gateway height (h_b) parameter is set to 30 meters and the node height(h_m) is set to 1.5 meters. The factor $a(h_m)$, given by (3.4) depends on the chosen environment and the chosen f_c, which in this case being a metropolitan area and with a $fc \geqslant 400MHz$,

$$a(h_m) = 3.2(log(11.75h_m))^2 - 4.97 \tag{3.4}$$

In order to calculate the MCL that the network would support, which is given by (3.5), where the P_{tx} represents the maximum allowed power in Europe of 14 dBm imposed by the ISM band [50] and S represents the sensibility of the gateway at room temperature - which is given by (3.6) - first it was required to know the characteristics of the system to be implemented.

$$MCL_{[dB]} = P_{tx} - S \tag{3.5}$$

$$S_{[dBm]} = -174 + 10log_{10}(BW_{[kHz]}) + NF + SNR \tag{3.6}$$

The first term represents the thermal noise in 1 Hz of the bandwidth, and can only be influenced by changing the temperature of the receiver. The BW is the receiver bandwidth, Noise Figure (NF) is the receiver noise figure (based on the hardware used) and the SNR is the value required by the modulation used (spread spectrum), determined by the SF. Proportionally, the higher the SF, the higher the absolute value of the SNR, as seen in Table 3.1.

Table 3.1: Spreading Factor and SNR variance [67].

Spreading Factor (SF)	SNR (dB)
7	-6
8	-9
9	-12
10	-15
11	-17.5
12	-20

As mentioned previously, the NF differs depending on the chosen equipment. Since there was no equipment set to be used in this dissertation, the value chosen to this parameter of 6 dB was done based on typical LoRaWAN implementations [68].

Then, depending on the selected parameters (BW and SF) the values on Table 3.2 for the sensibilities can be achieved, with values ranging from -117 dBm to -137 dBm.

Table 3.2: Sensitivity according to different spreading factors and bandwidth.

	Bandwidth (kHz)		
SF	125	250	500
7	-123.03	-120.02	-117.01
8	-126.03	-123.02	-120.01
9	-129.03	-126.02	-123.01
10	-132.03	-129.02	-126.01
11	-134.53	-131.52	-128.51
12	-137.03	-134.02	-131.01

Now, taking (3.1) and solving it for d, it is possible to calculate the Maximum Node Distance (MND) to the gateway, given by (3.7). The obtained values are further

discussed on subsection 3.2.1.

$$MND_{[m]} = 10^{\left(\frac{MCL-A}{B}\right)} \times 1000 \tag{3.7}$$

Having the MND figured out, this will serve as a baseline to place the gateway. The gateway placement in the network is done by setting it in space with the coordinates of MND, given by (3.8) and (3.9). The additional 10 meters added to the MND are meant to provide leeway for the nodes, in case there is a node placement in the edge of the maximum allowed distance. This is implemented because there is a rule of a minimum distance of 10 meters between nodes and/or the gateway. The imposed distance was chosen arbitrarily, and can be changed if needed.

$$GW_{x_m} = MND + 10 \tag{3.8}$$

$$GW_{y_m} = MND + 10 \tag{3.9}$$

3.1.2 Node Creation & Placement

This section covers the first part of this framework, the creation and placement of the node in the network. This is done by using an algorithm to sum a random generated float between 0 and 1 (3.10 and 3.11) and the previous calculated parameters (3.7, 3.8 and 3.9).

$$a = random.random() \tag{3.10}$$

$$b = random.random() \tag{3.11}$$

The x and y positions are then calculated (3.12 and 3.13).

$$Pos_x = b \times MND \times cos\left(2\pi\frac{a}{b}\right) + GW_x \tag{3.12}$$

$$Pos_y = b \times MND \times sin\left(2\pi\frac{a}{b}\right) + GW_y \tag{3.13}$$

The node placement is done in an iterative manner. Following a methodology of 100 tries to place the node, the Distance Between Nodes (DBN) must comply with a

minimum distance of 10 meters (as explained earlier), according to 3.14.

$$DBN_{[m]} = \sqrt{Pos_x^2 + Pos_y^2} \tag{3.14}$$

If the distance is smaller than the set distance between nodes (10 meters), the node is not placed and the total amount of node placement failures is increased by 1. If the total number of node placement failures reaches the 100^{th} mark, the simulation is canceled.

Granted the distance is compliant with the minimum needed, the Node Distance (ND) is defined as follows:

$$ND_{[m]} = \sqrt{(Pos_x - GW_x)^2 + (Pos_y - GW_y)^2} \tag{3.15}$$

Finally, having the node creation and placement configured, the next step is the creation of the packet itself.

3.1.3 Packet Creation

In this section the packet creation that each nodes carries is explained. In order to create the packet, some parameters are needed, such as: payload of each message, the ND (previously calculated in section 3.1.2) and the experiment type (i.e. the DRs further discussed on Table 3.4). The experiment type contains the values of the SF, CR, BW used for each group of devices. All of these parameters will dictate the behaviour of each group of devices regarding the airtime of the packets that are sent.

First, the MCL is calculated for each packet using (3.1), with the distance d previously estimated in (3.15). After having the value of the MCL for this node/packet, the P_{rx} by the gateway is then determined as follows:

$$P_{rx[dBm]} = P_{tx} - MCL \tag{3.16}$$

Then, using the given SF, CR and BW based on the experiment type, the airtime of each packet is calculated according to:

$$Airtime_{[ms]} = T_{preamble} + T_{payload} \tag{3.17}$$

with $T_{preamble}$ and $T_{payload}$ given by (3.18) and (3.19):

$$T_{preamble} = (N_{preamble} + 4.25) \times T_{sym} \tag{3.18}$$

$$T_{payload} = T_{payloadSymbNB} \times T_{sym} \tag{3.19}$$

In order to achieve the above equations, more detail is needed. The $N_{preamble}$ parameter is typically set to 8 symbols in LoRa networks, to each the system adds 4.25 symbols, as depicted in Figure 2.6. The T_{sym} (3.20) is determined based on the SF and BW settings as follows:

$$T_{sym} = \frac{2^{SF}}{BW} \tag{3.20}$$

The $T_{payloadSymbNB}$ given by (3.21) uses as parameter the chosen payload size, SF, CR and the H and DE flags. The H flag stands for the implicit header and by default is set to 0 (not active). This can be changed to 1 (active) if needed, although the SX1272/73 transceiver from Semtech is configured to automatically set the implicit header mode to active when the SF used is 6. The DE flag stands for low data rate optimization, and by default is also set to 0 (not active). This can also be set do active if needed, although is automatically set to active when used with BW125 and SF11/SF12 settings.

$$T_{payloadSymbNB} = 8 + \frac{8 \times payloadsize - 4 \times SF + 28 + 16 - 20 \times H}{4 \times (SF - 2 \times DE)} \times (CR + 4) \tag{3.21}$$

Having the packet created, there is the need to implement a collision model to represent packet collisions during transmission, as explained in section 3.1.4.

3.1.4 Collision Model

This section explains how the collision model is implemented in the simulator. There are three versions presented in this dissertation: a simple version that checks the frequency and the spreading factor of the packets on the gateway, a capture effect that used the Received Signal Strength Indication (RSSI) between packets to ascertain if there is a collision or not, and a more complex method using a capture-effect that depicts a non-destructive approach based on probability as an alternative to the regular 0 dB (destructive mode) system.

3.1.4.1 Destructive Mode (0 dB)

In a pure-ALOHA network using the 0 dB method, every packet that arrives at the gateway is subject to a simplified collision check. Two transmissions that overlap in time but use a different CF do not collide, if the receiver is listening to both frequencies and the designated threshold between the packets frequency is respected. In this case, both packets are able to be decoded. The same can be applied to SF: transmissions with distinct SF values are orthogonal to each other which enables multiple signals to be transmitted at the same time. The simplest method to make this validation is through the frequency and spreading factor analysis of both packets.

According to [69], two packets collide in the frequency domain when:

$$Collision_{Freq} = \begin{cases} |f_1 - f_2| \leqslant 120 \text{ kHz and } BW_1 \text{ or } BW_2 = 500 \text{ kHz} \\ |f_1 - f_2| \leqslant 60 \text{ kHz and } BW_1 \text{ or } BW_2 = 250 \text{ kHz} \\ |f_1 - f_2| \leqslant 30 \text{ kHz and } BW_1 \text{ or } BW_2 = 125 \text{ kHz} \end{cases} \tag{3.22}$$

In the case of similar SF between packets (i.e. non-existence of orthogonality between the packet's SF), they are flagged for collision. Therefore, two packets collide in the SF domain when (3.23):

$$Collision_{SF} = \begin{cases} True, \text{if } SF_{packet1} = SF_{packet2} \\ False, \text{if otherwise} \end{cases} \tag{3.23}$$

If both packets prove to have frequency and spreading factor collision simultaneously, these are considered lost.

3.1.4.2 Capture-Effect - 6 dB Mode

In the 6 dB capture-effect approach, besides the steps taken in the 0 dB method (subsection 3.1.4.1) there is also an additional two step validation to the packets on the gateway. The first step is to check for concurrent transmissions. A concurrent transmission imply that two or more packets coming from devices that are configured with the same parameters overlap in time, thus leading to frame collisions and consequently to packet loss, as depicted in Figure 3.1. Assuming that the number of symbols on the preamble ($N_{preamble}$) is 8, as discussed previously on subsection 3.1.3, that means that

we can only lose 3 symbols multiplied by the period of said symbol:

$$T_{Limit} = T_{Sym} \times (N_{Preamble} - 5) \tag{3.24}$$

Then calculating the total amount of time of the packet that arrived first at the gateway (3.25) and comparing with the critical section of the last packet that arrived (3.26), it is possible to conclude if the last packet that arrived is going to be processed or if it is going to be lost.

$$T_{FirstArrivedPacket} = T_{ProcessedTime} + T_{Airtime} \tag{3.25}$$

$$T_{CriticalSection} = T_{ReceivedTime} + T_{Limit} \tag{3.26}$$

The $T_{ProcessedTime}$ variable reflects the time that the gateway took to process the packet. Adding it to the total airtime of said packet, its possible to have an estimation of the time for the first packet that arrived.

The $T_{ReceivedTime}$ represents the time of arrival of the last packet to the gateway. This added to the tolerance period calculated on (3.24) generates the critical section which dictates if the second packet is rejected or not.

After calculating the above variables, there is a simple check to verify if a timing collision between the concurrent transmissions occurs:

$$Collision_{Timing} = \begin{cases} True, \text{if } T_{CriticalSection} < T_{FirstArrivedPacket} \\ False, \text{if otherwise} \end{cases} \tag{3.27}$$

If there is a timing collision between the packets, then the second step of the validation occurs. The second step is to evaluate on the power domain. According to [50] a packet can be decoded during a collision if the difference in the received RSSI is higher than a certain threshold value, in this case set to 6 dB. Depending on the difference in power between the packets, multiple things can occur:

$$Collision_{Power} = \begin{cases} |RSSI_1 - RSSI_2| < P_{Threshold}, \text{both packets are lost} \\ RSSI_1 - RSSI_2 < P_{Threshold}, Packet_1 \text{ is decoded} \\ RSSI_1 - RSSI_2 > P_{Threshold}, Packet_2 \text{ is decoded} \end{cases} \tag{3.28}$$

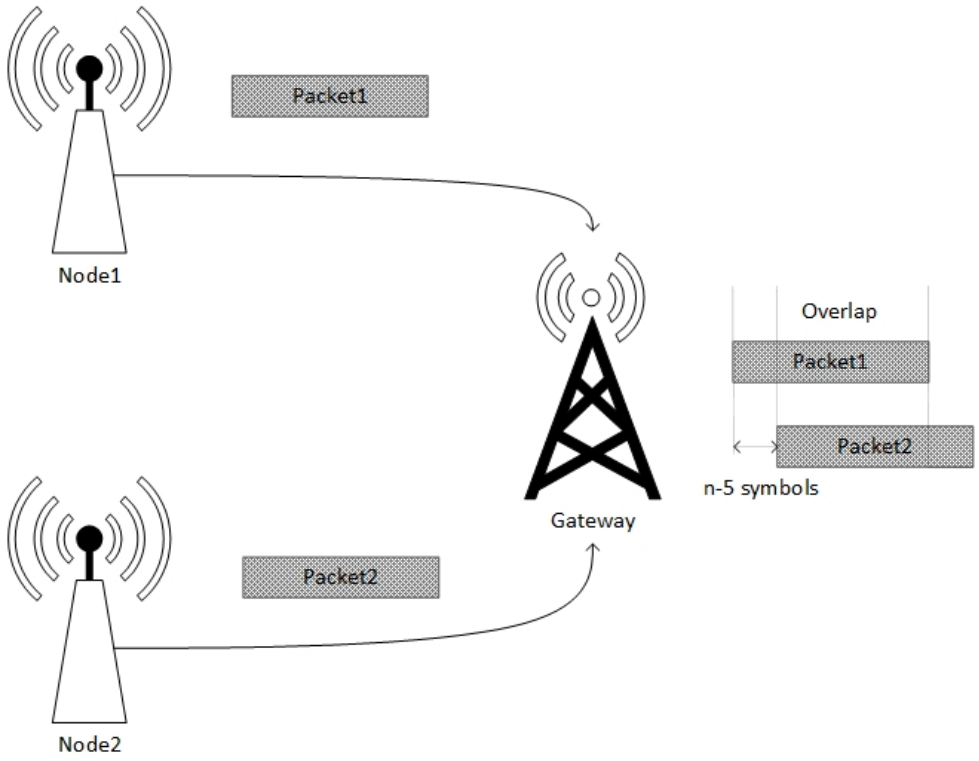

Figure 3.1: Packet collision example.

3.1.4.3 Capture-Effect - Non-Destructive Method

However, this evaluation on the power domain is not considered the best approach to follow when trying to identify a collision. In [63] it was developed a more realistic model for the capture effect.

Using a anechoic chamber as a controlled environment to study synchronized transmissions, some results were achieved. The use of this chamber provided stable RSSI values over multiple transmissions, which is the point of interest in the coming conclusions for concurrent transmissions analysis. Assuming that each end-node is static and without multi-path fading, this outcome depicts the best case scenario for the network capacity.

Despite the values for the RSSI of the nodes presented on Table 3.3 are not necessarily the same for this dissertation (because on this analysis attenuators were used to achieve this range of values, while on this dissertation none were used), the results for the Frame Error Rate (FER) depending on RSSI gap between the packets still holds true, as claimed by the authors after repeating the tests for several times with different sets of RSSI values. In short, the absolute values of the RSSI for each packet are not relevant, only the gap between the two.

Table 3.3: Frame Error Rate based on RSSI gap between packets [63].

RSSI of weakest node [dBm] \ RSSI gap [dBm]	5	3	2	1	0
-100	4%	4%	21%	38%	75%
-105	0%	2%	20%	36%	74%
-110	6%	2%	17%	38%	68%
-115	6%	4%	19%	43%	70%
-120	2%	2%	14%	41%	66%
Average	4%	3%	18%	39%	71%

Assuming that every node is on the same conditions (i.e all the packets of each node are received with the same RSSI by the gateway), some conclusions can be attained by analyzing table 3.3:

- When both transmissions have the same RSSI, there is an average of 71% chance of losing both packets, and a 29% chance of one being processed;
- When there is a RSSI gap of 1 dBm, there is a 39% chance of losing both packets and a 61% chance of the strongest packet arriving being processed;
- When there is a RSSI gap of 2 dBm, there is a 18% chance of losing both packets and a 82% chance of the strongest packet being processed;
- When there is a RSSI gap of 3 dBm, there is a 3% chance of losing both packets and a 97% chance of the strongest packet being processed;
- When there is a RSSI gap of 5 dBm, there is a 4% chance of losing both packets and a 96% chance of the strongest packet being processed.

According to these results, the following approximation was obtained:

$$1 - FER \approx \prod_{J \in j} 1 - FER_j \tag{3.29}$$

where J represents the set of interfering nodes, and FER_j represents the FER observed when two concurrent transmissions are observed between the weakest node j and the reference node (the one being analyzed by the algorithm at a given moment).

3.1.5 Energy Consumption Model

This section has the purpose to provide a brief insight of how the energy consumption of the network (also known as the Network Energy Consumption (NEC)) is

calculated.

The total energy spent by the network is very important to the long-term performance and durability. Since the nodes are largely deployed relying on batteries, it is essential to keep the energy consumption for the transmissions to a minimum. The energy consumption for each transmitted message relies on the TP and the airtime, which is influenced by the SF, BW, CR.

As seen on (3.30), the total amount of energy spent by the network is calculated using each packet airtime (from 1 to n, which represents the number of sent packets), the electric current equivalent for the used TP (which in this case for the fixed 14 dBm used its the equivalent of 44 mA for all packets, according to the LoRaSim authors) and a fixed voltage of 3 V, for all the packets that were successfully sent. Similarly to the distance between nodes explained on subsection 3.1.1, these parameters can be changed if needed.

$$Energy_{[J]} = \frac{\sum_{i=1}^{i=n} nodePacketAirtime(i)_{(ms)} \times TxConsumption_{(mA)} \times V}{1 \times 10^6} \tag{3.30}$$

In short, the NEC depends on the number of packets that are sent, frequency of transmissions and transmitter communication parameters as seen above. The lower the metric, the more efficient is the deployment as the lifetime of the nodes is longer. The energy required to extract a message should be independent of the number of nodes deployed in the network, since it analyses each node individually. Again, the metric does not capture individual node behaviour and is a metric looking at the network deployment as a whole.

3.2 Simulation

In this section some results are displayed, namely the differences that occur when changing the mode used for the system, the propagation model, and the pure-ALOHA destructive properties against the 6dB method and a non-destructive method.

As seen on (2.2), the DR is determined by the chosen settings (SF, BW, CR). There is also the P_{tx} value that plays a role on the DR of the system, but it is not a variable since due to regulatory constraints and battery life issues this value is capped to a maximum of 14 dBm on the sub-band used on this dissertation.

On Table 3.4 are 4 examples of settings that can be used in a LoRaWAN network.

The use of these modes presuppose the absence of the ADR (i.e., the devices assume one mode and are not changed or adapted during the simulation process).

The mode 0 is the fastest setting available, while the Mode 3 is the slowest. The mode 1 and 2 are two examples of the many configurations that can be used, each one applied to different circumstances. For instance, if a node is far from a gateway, then the slowest mode should be used (mode 3), because it provides the best protection against noise. On the other hand, if the node is close to the gateway, then the fastest configuration should be used (mode 0).

Table 3.4: Example of LoRaWAN Data Rates.

Mode	Bandwidth (kHz)	Spreading Factor	Code Rate (4/(CR+4))	Data Rate (bps)
0	500	7	4/(1+4)	21875
1	250	9	4/(1+4)	3516
2	125	12	4/(1+4)	293
3	125	12	4/(4+4)	183

First some results showing the differences between the two propagation methods used (log-distance and OH) will be showcased. Then, some results analyzing the quality of the network depending on the settings used will be presented. Finally, the differences among the 0dB setting (destructive mode), capture-effect (6 dB method) and the non-destructive approach based on probability, will be discussed.

3.2.1 Propagation Model

In this subsection some experiments are made comparing both propagation models. On one hand, there is the log-distance model that the original developers of Lorasim used, based on their own empirical measurements. On the other hand, there is the generic Okumura-Hata propagation model, which was used precisely to not bound to any set up environments or empirical measurements.

Using the mode 2 on Table 3.4, an analysis was performed to compare the behaviour of the network when using each of the propagation models. On Figure 3.2 it is possible to see the variation of the RSSI using the log-distance propagation model. The maximum distance allowed using the empirical variant of the LoRaSim developers is nearly 100 meters, which is clearly unrealistic for LoRa communications. The curve is similar to a exponential decay, meaning that the furthest the distance from the gateway, the greater is the loss of the RSSI.

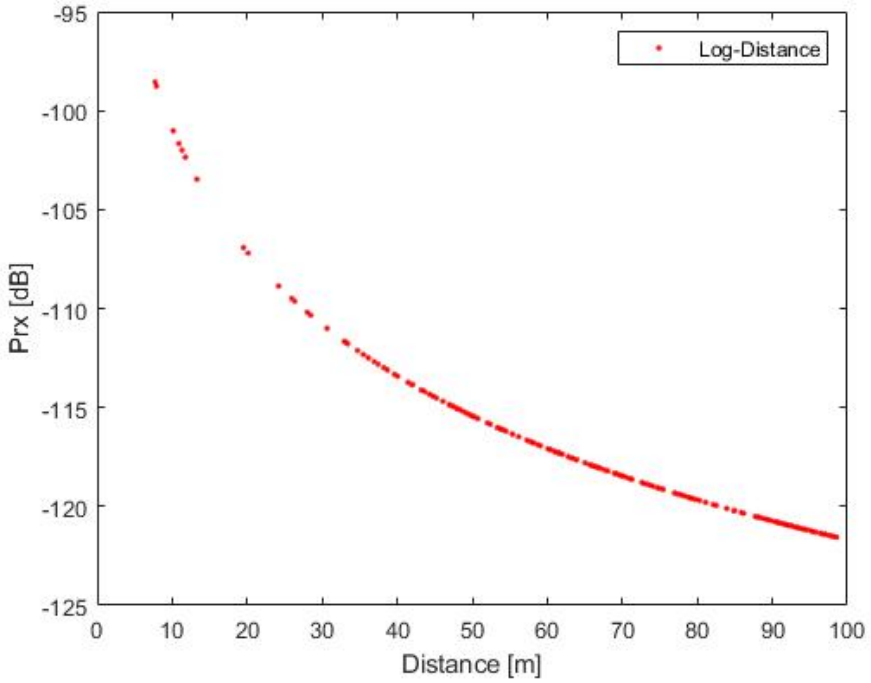

Figure 3.2: Receiver power variation using the log-distance propagation model.

On Figure 3.3 the same analysis is performed, but now using the OH propagation model instead. The main difference from the previous figure is the maximum distance that is allowed in the network. Using this propagation model we get more than 40 times the coverage of the original method, while maintaining acceptable RSSI values.

Taking the first 100 meters as a reference for both propagation models, some conclusions can be drawn when analysing Figure 3.4. Since the simulator randomly places the nodes on the network (as seen on subsection 3.1.2), there was the need to do an extrapolation of the data for the range of [0,100] meters for both propagation models. As expected from the two previous analysis, when looking into detail for this range of distance, there is a much higher decay on the RSSI for the log-distance propagation model. This is correlated to the much higher available distance for the network on the OH propagation model, which is the main strength that lead to picking it for the used propagation model of this dissertation.

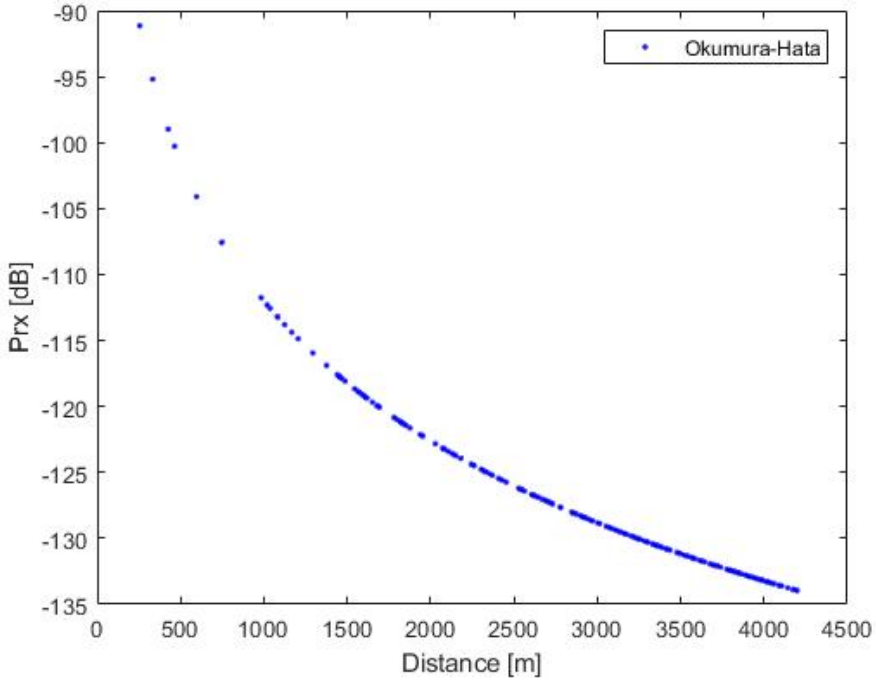

Figure 3.3: Receiver power variation using the Okumura-Hata propagation model.

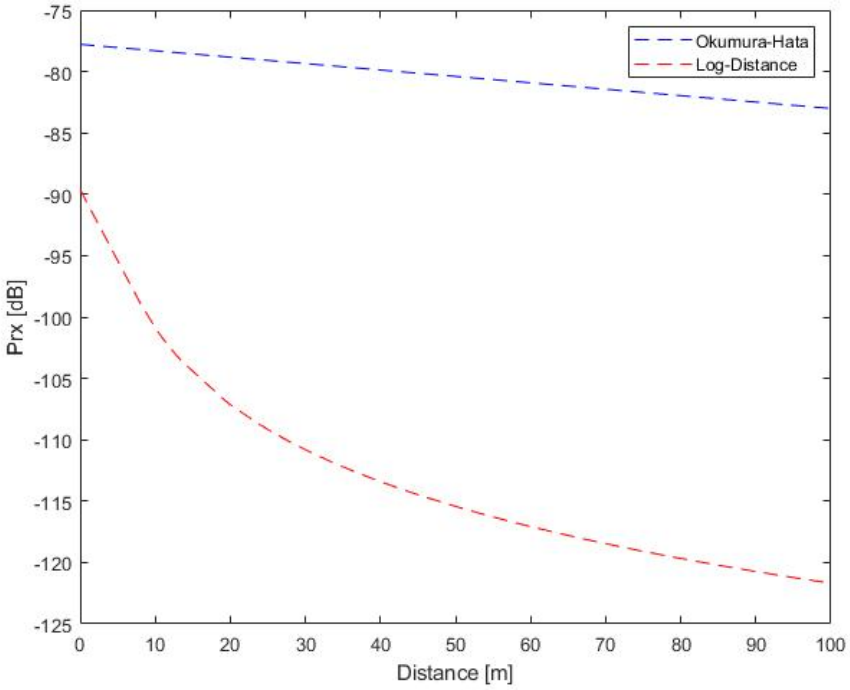

Figure 3.4: Receiver power variation of both propagation models for the first 100 meters range.

3.2.2 Enhanced Simulator

One perk of this simulator over the original LoRaSim is the option to set different parameters for each group of nodes. This offer the advantage of planning the network according to the distance that each group of nodes are relatively to the gateway.

This feature enables more flexibility to the network. By choosing different parameters the network automatically improves, since there is more orthogonality between the sent packets, hence diminishing the overall collisions while using the energy in a more optimized way due to the available resources. Using Table 3.4 as reference for a setup environment, an analysis was performed using 4 groups each with their own mode against a network using just one group of nodes, with the same mode among them. All the simulations are done varying the number of nodes in the network, resulting in different networks (i.e., network 1 has 100 nodes, network 2 has 200 nodes, all the way until network 10 with 1000 nodes).

Besides the aforementioned parameters used, for the environment created for this simulation the following parameters were also defined:

- **Propagation model:** Both scenarios used the same propagation model for a better analysis of the differences between simulators. The model used was the Okumura-Hata;
- **Payload:** A fixed payload of 20 Bytes on both cases was used;
- **Average send time between packets:** Each mode has its own average time between packets, calculated according to the airtime (3.17) and the duty cycle of the network (2.3). The duty cycle of 1% is used for all cases:

  Mode 0: 1 seconds (1414 *ms*);

  Mode 1: 9 seconds (9267 *ms*);

  Mode 2: 2 minutes and 12 seconds (131891 *ms*);

  Mode 3: 2 minutes and 51 seconds (171213 *ms*).

- **Simulation Time:** 10 days (the equivalent of 864.000.000 *ms* of simulation run time).

On Figure 3.5 it is depicted the node group placement based on the selected parameters for a network of 1000 nodes. In this case, the center dot represents the gateway, and the color dots represent each group of nodes. The nodes closest to the gateway (blue) express the quickest mode (mode 0), by trading distance for speed. Inversely, the farthest nodes (red and black) represent the slowest modes (mode 2 and

mode 3). The nodes in pink can be considered as a middle ground, as they offer a compromise between distance and speed (mode 1). At the same time, the groups that have the highest flexibility in distance (black and red groups) are the ones that can be more easily scattered around the network, as the nodes can pretty much operate under any distance to the gateway without any loss of packets. This is seen by having these groups not only far from the gateway but also near it.

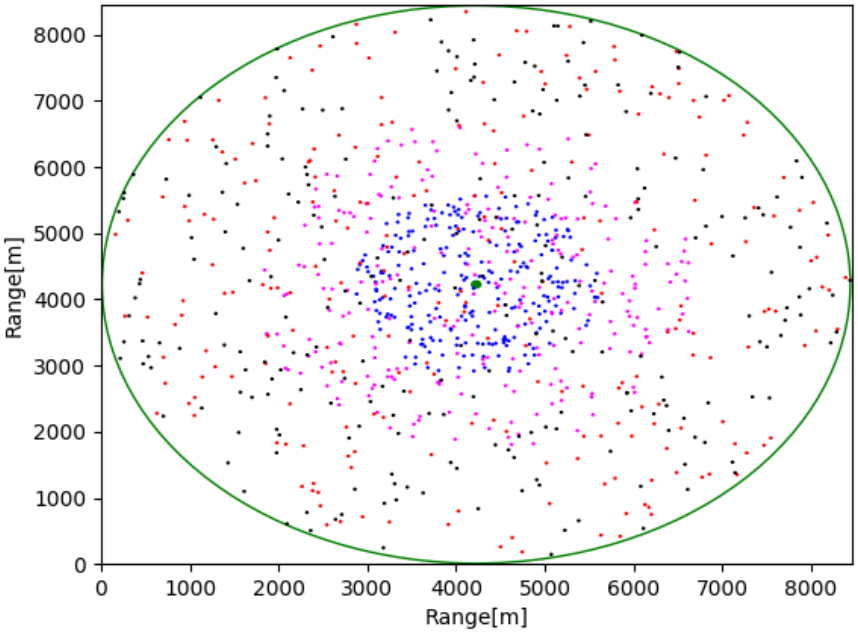

Figure 3.5: Node placement in the network according to the group parameters.

On Figure 3.6 there is an analysis of the network DER between both circumstances. As covered previously, a network in perfect condition would have a DER of 100%, that would translate to having all the sent packets received by the gateway successfully.

On one side of this analysis is a simulation using the 4 modes presented on table 3.4, designated as **enhanced LoRaSim configuration**. While this configuration does not replace the use of a more complex technique such as the ADR and since this dissertation doesn't cover the use of it because it is offered by the network server, the idea of using different parameters according to the distance of the nodes to the gateway arose. There are four groups of nodes where each group uses one mode, allowing the simulation of a realistic scenario where all the nodes present different distances to the gateway, therefore not needing to use the same mode. The network acts as expected, showing a decay on the overall quality of the network according to the increase of the number of devices.

On the other side, there is the simulation mimicking the standard LoRaSim configuration, designated as the **original LoRaSim configuration**. This network simulated using the method that the original LoRaSim had, enforced the need to assume one mode for the entire network, due to the lack of flexibility. In this case, the mode 3 was used since its the one that trades speed with distance, offering the greatest transmitting distance of all presented in this analysis.

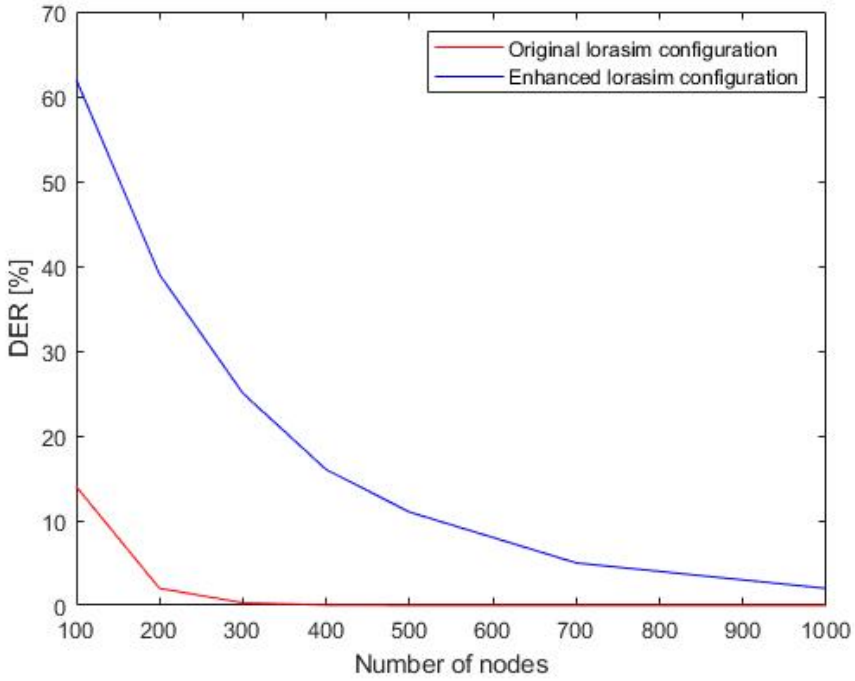

Figure 3.6: Network quality between the original LoRaSim and the enhanced variant.

Comparing both approaches when trying to design a network, it is visibly more realistic to use the enhanced version of the LoRaSim instead of the original version. When analysing the first 100 nodes of the network, there is an increase of 47% in the DER value (62% against 15%), while at the 300 nodes or above, the DER value of the original LoRaSim is 0% and the enhanced version still holds relevancy: 25% at 300 nodes decaying to 2% when reaching the 1000 nodes.

On Figure 3.7 there is a comparison of the energy consumption for both networks. Following the energy estimation determined on subsection 3.1.5, it is visible that both curves are akin to a linear behaviour. Overall, the energy spent by both networks are the same. This happens because there is a better use of the network energy in the enhanced version. By having different data rates on the network, there is a better use of the energy that each group of nodes spend according to the distance that they are from the gateway.

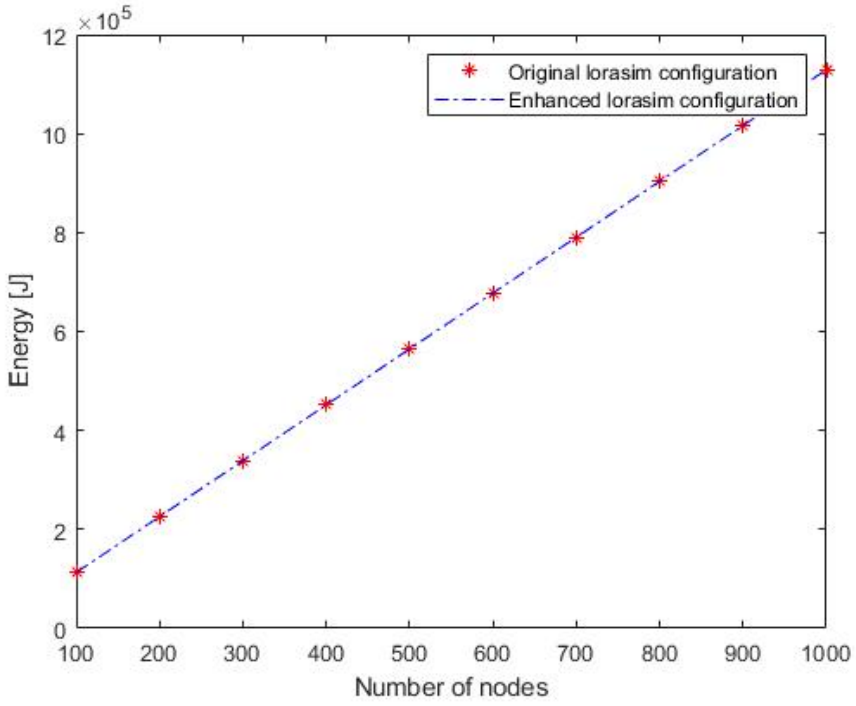

Figure 3.7: Energy consumption between the regular LoRaSim and the enhanced variant.

When looking to Table 3.5 portraying the total amount of sent packets, total collisions and total energy spent by both systems with 1000 nodes each, it is possible to see that when comparing both simulators under the same circumstances (same mode) the amount of packets transmitted is inferior on the enhanced LoRaSim, while the energy spent is roughly the same. This happens because on the enhanced LoRaSim there are other data rates (in this case also faster than the mode 3 used by the original simulator) that are transmitting simultaneously, greatly increasing the total number of packets sent by the network, thus increasing the total energy spent of the system. As seen previously on Figure 3.6, the choice of having a network with multiple data rates according to the distance results in a better network DER, while spending the same amount of energy that the original LoRaSim does (Figure 3.7). This makes the network more optimized regarding the available resources to it.

Going forward, now all modes of Table 3.4 will be used for the study of the non-destructive mode introduced in subsection 3.1.4.3. As previously said, this method has the capability of increasing the network quality by a good margin. On Figure 3.8 its possible to see that when applying the non-destructive mode there is an improvement in quality when comparing to the 0 dB network approach. This happens because there is a probability that when a packet arrives to the gateway and collides to another, there is still a chance that both might be processed, decreasing the total amount of collisions

Table 3.5: Comparison between simulators for a network of 1000 nodes.

	Enhanced LoRaSim		Regular LoRaSim	
Mode	Sent Packets	Total Collisions	Sent Packets	Total Collisions
0	151.230.869	148.795.014	—	—
1	23.082.651	21.472.074	—	—
2	1.622.154	1.602.450	—	—
3	1.248.935	1.244.862	4.991.877	4.991.877
Total Packets	177.184.609	173.114.400	4.991.877	4.991.877
Total Energy (J)	1.129.384		1.128.168	

in the system and increasing the DER value.

On Table 3.6 it is presented a full network analysis comparing both approaches to the network, using the ten networks simulated previously as reference. It is possible to see that the amount of collisions for the 0 dB network is superior to the amount of collisions by the non-destructive approach. As seen on Figure 3.8, this results in a higher DER value for the non-destructive mode, representing on average an increase of 28,5% across all networks when using the non-destructive network.

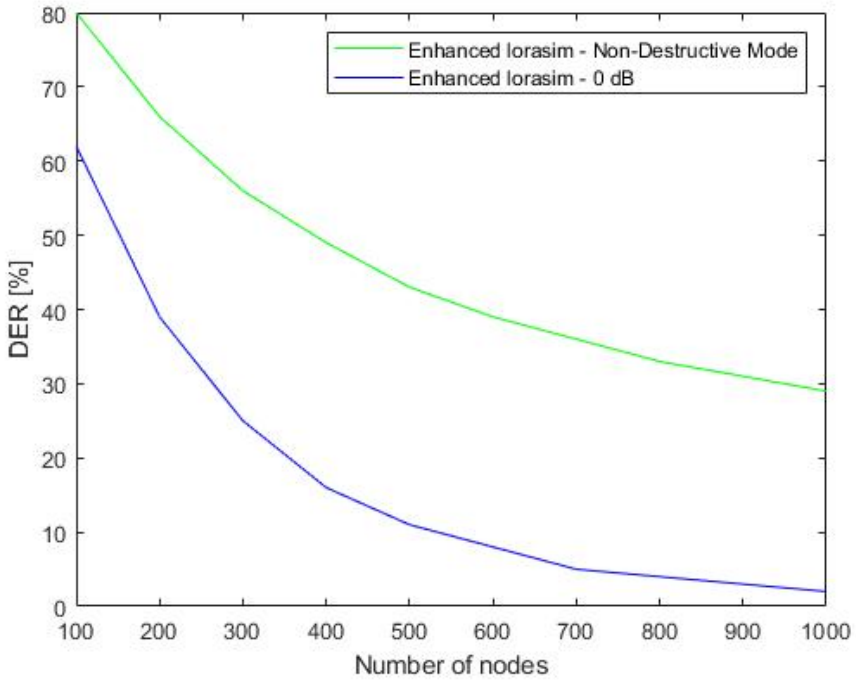

Figure 3.8: Network quality between the 0 dB and non-destructive mode.

When comparing the non-destructive mode method as a capture-effect with another well-known method (the 6dB threshold), there is still a large difference. Figure

Table 3.6: Comparison between 0 dB and non-destructive mode.

	0 dB			Non-Destructive		
# Nodes	Sent Packets	Total Collisions	DER	Sent Packets	Total Collisions	DER
100	17.717.821	6.658.373	62%	17.714.802	3.384.310	80%
200	35.440.866	21.486.225	39%	35.433.855	11.719.132	66%
300	53.162.921	39.602.359	25%	53.159.450	22.936.533	56%
400	70.865.523	58.834.809	16%	70.860.544	35.841.545	49%
500	88.597.007	78.337.749	11%	88.604.282	49.780.995	43%
600	106.314.006	97.720.921	8%	106.316.719	64.296.442	39%
700	124.047.217	116.905.956	5%	124.054.582	79.316.286	36%
800	141.761.867	135.842.166	4%	141.776.470	94.490.610	33%
900	159.476.769	154.570.190	3%	159.479.352	109.884.379	31%
1000	177.184.609	173.114.400	2%	177.190.995	125.311.123	29%
Average	97.457.000	88.307.000	17,5%	97.459.000	59.696.000	46%

3.9 depicts the differences among the 3 variants.

The 6dB approach presents itself as an improvement to the 0 dB mode. This is because, as seen in (3.28), if there is a collision on the other domains (frequency, spreading factor and timing) the difference in power between the interfering packets is what decides if a packet is decoded or if both will fail. This means that there is another layer of decision before discarding the colliding packets.

However, the non-destructive mode presents itself as a even better improvement as a capture-effect when compared to the 6dB method. This happens because there is a more detailed breakdown on the non-destructive approach than in the 6dB method. As seen on Table 3.3, the analysis performed on the packets by the non-destructive mode is done by splitting the RSSI into brackets, giving a probability to the interfering packets to survive depending on the difference of power between them. This allows for a deeper dissection of each collision, increasing the overall quality of the network.

Table 3.7 provides a recap of the three methods previously presented. The sent packets of the 6dB mode can be estimated to be roughly the same as the others, as seen previously by the negligible difference between the 0 dB and the non-destructive mode. Therefore, it is excluded from this analysis.

Analyzing the average of collisions and DER across all ten networks, there is a decrease of the total collisions of the system when comparing the 0 dB to the 6dB method, which leads to an increase of 6,4% in average to the network quality.

Comparing the 6dB method to the non-destructive mode, there is on average an increase of 22,2% when using the non-destructive approach, which is almost the double of the DER value for the 6dB method, on average. Using a direct comparison between

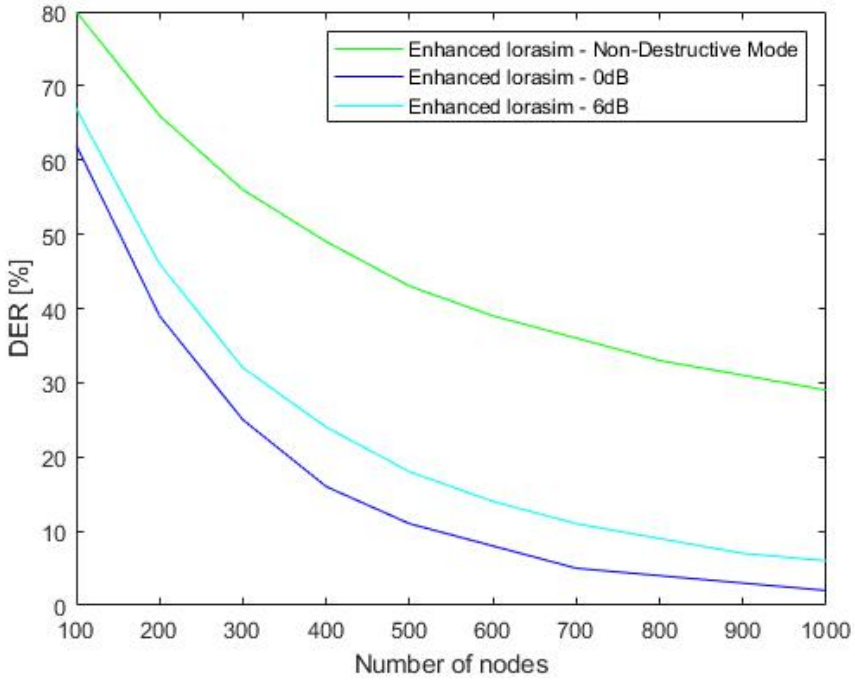

Figure 3.9: Network quality between the 0 dB, non-destructive mode and 6dB capture-effect.

networks, it is possible to see that the gap in network quality between the two methods increases as the network expands, as seen for example the difference between the 100 nodes and 1000 nodes networks, where there is a disparity of 13% for the 100 nodes network, and 23% on the 1000 nodes one.

Table 3.7: Comparison between 0 dB, non-destructive and 6dB capture-effect variants.

	0 dB		6dB		Non-Destructive	
# Nodes	Total Collisions	DER	Total Collisions	DER	Total Collisions	DER
100	6.658.373	62%	5.752.868	67%	3.384.310	80%
200	21.486.225	39%	18.821.043	46%	11.719.132	66%
300	39.602.359	25%	35.927.526	32%	22.936.533	56%
400	58.834.809	16%	53.660.321	24%	35.841.545	49%
500	78.337.749	11%	72.288.260	18%	49.780.995	43%
600	97.720.921	8%	91.369.035	14%	64.296.442	39%
700	116.905.956	5%	109.913.764	11%	79.316.286	36%
800	135.842.166	4%	128.478.435	9%	94.490.610	33%
900	154.570.190	3%	147.381.427	7%	109.884.379	31%
1000	173.114.400	2%	165.486.566	6%	125.311.123	29%
Average	88.307.000	17,5%	82.908.000	23,8%	59.696.000	46%

3.2.3 Network Capacity

The previous network configurations that were studied result on different network capacities. Studying each one and the respective impact of the network is the goal of the following analysis.

The analysis started with a comprehensive capacity assessment for networks of different scales, ranging from 0 to 1000 nodes, considering distinct packet sizes (payloads of 10, 20, 100 and 200) and different packet collision models: destructive mode (0 dB), capture effect (6 dB) and the probabilistic model (non-destructive).

As done previously on subsection 3.2.2, there was the need to calculate the average send time between packets for each mode. All simulations used the OH as a propagation model and 10 days for simulation time:

- **Average send time between packets:** Each mode has its own average time between packets, calculated according to the airtime (3.17) and the duty cycle of the network (2.3). The duty cycle of 1% is used for all cases:
  - **10 bytes payload:**
    Mode 0: 1 seconds (1030 *ms*);
    Mode 1: 7 seconds (7219 *ms*);
    Mode 2: 1 minutes and 39 seconds (99123 *ms*);
    Mode 3: 1 minutes and 59 seconds (118784 *ms*).
  - **20 bytes payload:**
    Mode 0: 1 seconds (1414 *ms*);
    Mode 1: 9 seconds (9267 *ms*);
    Mode 2: 2 minutes and 12 seconds (131891 *ms*);
    Mode 3: 2 minutes and 51 seconds (171213 *ms*).
  - **100 bytes payload:**
    Mode 0: 4 seconds (4358 *ms*);
    Mode 1: 28 seconds (27699 *ms*);
    Mode 2: 6 minutes and 34 seconds (394035 *ms*);
    Mode 3: 9 minutes and 51 seconds (590643 *ms*).
  - **200 bytes payload:**
    Mode 0: 8 seconds (7942 *ms*);

Mode 1: 50 seconds (50227 *ms*);

Mode 2: 12 minutes and 2 seconds (721715 *ms*);

Mode 3: 18 minutes and 35 seconds (1114931 *ms*).

In order to calculate the total capacity of each network for each configuration, the following was used:

$$NetworkCapacity_{[bytes/hour]} = \frac{ReceivedPackets \times PayloadSize}{SimulationTime_{[days]}} \times \frac{1}{24hours} \tag{3.31}$$

where the received packets is the difference between sent packets, collided packets and lost packets. After calculating all the capacities for the presented networks, some conclusions could be draw.

On Figure 3.10 it is possible to see the capacities for 10 networks (100 to 1000 nodes) for each collision mode. By increasing the payload size , the overall capacity of the network also increases, regardless the collision mode used. The 0dB and the 6dB show a decay at the 200 and 300 nodes networks respectively, while the non-destructive mode shows an increasing behaviour resembling an logarithmic curve.

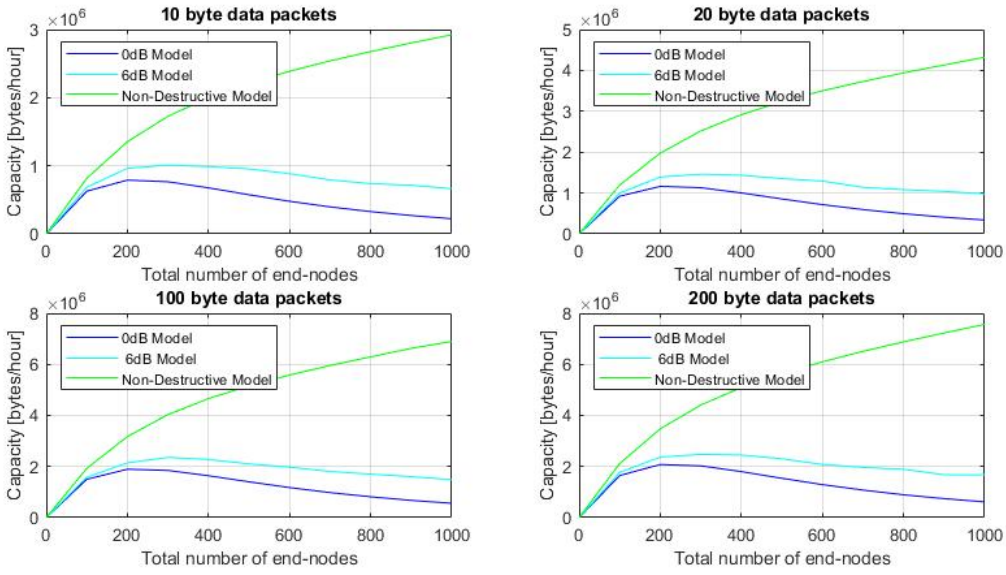

Figure 3.10: Network capacity for different networks and different packet payloads.

Due to the probabilistic model of the non-destructive mode enabling a optimistic approach to the packets received and the fact that the network operates with 3 modes that are orthogonal (since the only difference between mode 2 and 3 is the CR, there are only 3 modes that share orthogonality among them - Mode 0, 1 and 2) this, together

with the fact that there is not any loss of packets since the minimum RSSI from the nodes to the gateway is guaranteed, represents an higher network capacity the higher the number of nodes in a network. Simply put, more packets sent equals to more packets received, despite the collisions on the network.

However, this does not mean that the capacity is infinite nor the network is performing well. As seen before (Figure 3.9), the DER value is the metric that evaluates the quality of the network, and it decreases in quality with the increasing of the total amount of nodes in the network. It is not possible to see the throughput of the network by simply looking into the capacity, since it goes hand to hand with the DER value of the network. As an example, if the network has a throughput of over 1.000.000 packets in a hour but has a input of 10.000.000 packets and consequently a low DER value, then the network is performing poorly.

In theory, to ascertain the limit in capacity for a network with this parameters, the maximum nodes supported by a network would need to be reached.

To prove the aforementioned, Figure 3.11 depicts the network capacity for networks with only one group, on mode 0 which is the fastest group among the four modes on this dissertation, enabling a higher transmission of packets on the network and consequently a higher amount of collisions as well. Here we see that the behaviour of the networks follow the expected: by using a single mode there is no orthogonality among the received packets, fostering the increase of the collisions in the system.

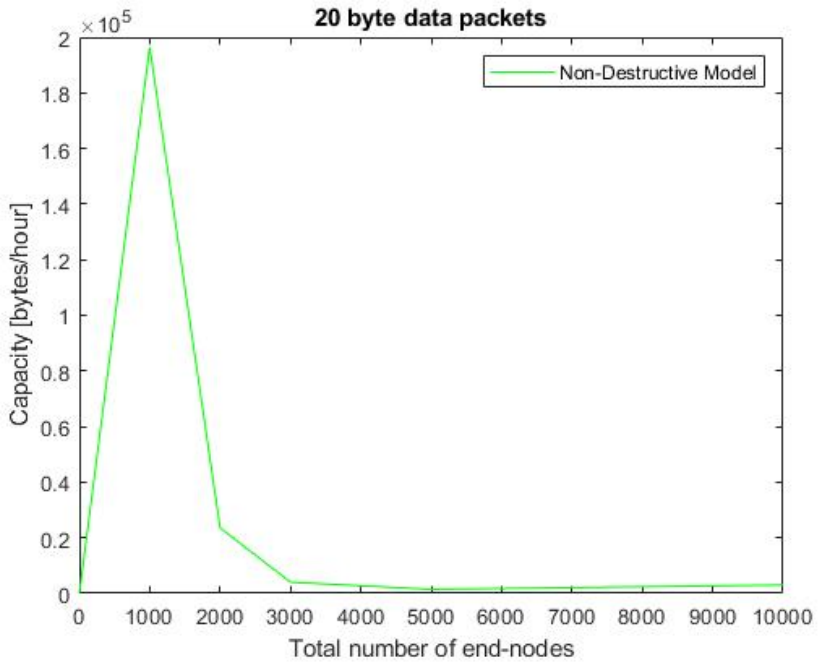

Figure 3.11: Network capacity for different networks.

3.3 Chapter Considerations

This chapter initially presented the simulator architecture - the logic behind the procedure of gateway and nodes placement - and the three collision models used and their differences. Also, results were shown with the differences between the collision models used and the network capacity.

First, the decision to use the OH as a propagation model was explained, as well as all the parameters that were needed to calculate the MCL. Having the MCL value, the maximum distance that the nodes can be placed is calculated, as well as the location of the gateway position. After that, the node creation and placement following the designated criteria is conducted.

Furthermore, having the network infrastructure already built, the packet creation was taken in motion. The first stage was to determine the P_{rx} that the gateway will receive based on the node position (calculated with the MCL). In order to create the packets, some equations that resemble the logic are presented. As seen, the airtime of the packets are calculated using the preamble and payload values, which in turn are intrinsically dependent of the chosen parameters (SF, BW, SF, CR and payload values) for each group in the network. Lastly, the energy consumption model of the network was presented and it functionality explained.

Then, the collision models that are offered as options for the simulator are conferred. The logic behind the way how the collisions are handled is showcased, for the 0 dB (destructive), 6dB (capture-effect) and probabilistic model (non-destructive).

Moreover, simulations are performed using four different modes with distinct data rates. First the differences between the two propagation models are presented, where the choice for the use of the OH is also explained and demonstrated through the results obtained. Afterwards, more simulations and breakdown analysis are achieved to exhibit the network behaviour and the differences between all the collision methods available in this dissertation, regarding the quality of the networks that can be accomplished with each method used.

Finally, the network capacity is measured according to payload used. The capacity offered by the three collision models are compared. Results have shown that the probabilistic model has a higher capacity than the other two models, due to the optimistic approach that this model uses. It is explained that despite the good performance in the capacity subject, the overall network quality gets poorer the more nodes the network has. An example of a network purely with the non-destructive mode is given to

explain how the packets behave when there are four modes versus when there is only one mode across all nodes in the network.

The next chapter presents an analysis of a smart city deployment using the simulator developed in this dissertation, discussing the choice of devices and gateway placement when planning an IoT network based on LoRa communications.

4

Smart City

This chapter describes the process of planning smart city sensor network based on LoRa by taking advantage of the changes made to the simulator, namely the option to configure multiple groups of nodes, the changes to the used signal propagation and capture-effects models, studied on chapter 3. Section 4.1 shows the simulation environment, by explaining the steps taken to simulate a smart city using the proposed simulator. Section 4.2 presents the results of different simulation scenarios, by varying the operating modes and number of devices in the network, either gateways or end-devices. Finally, Section 4.3 summarizes the chapter contributions.

4.1 Simulation Environment

As previously seen on chapter 3, several changes were made to the LoRaSim simulator. However, in order to be be able to simulate a smart city, more development on the simulator was needed.

The idea was to create a tool to allow the user to plan a network in two steps:

- Determine the total number of nodes in the city, divided by groups, where each group has the liberty to have any DR that the user may wish to configure. For simplicity sake, in this analysis the four modes presented on table 3.4 will be

used to describe the devices in the network. This behaviour resembles the heterogeneity of devices that compose a smart city, where there are devices for every purpose, each with a certain DR, randomly spread around the city;

- After having a map drawn with the locations of every nodes in the network with their respective coordinates, the user can then decide where to place the gateway(s) in the city.

To be able to achieve this, the simulator was split into two different processes.

The planning process takes as an input the amount of groups and number of devices for each group. The result is shown as a map with all the nodes randomly spread around the network, where each group has its own colour depending on the DR. According to this, there is a maximum distance that each group can have from the gateway without suffering from any loss of packets due to the insufficient RSSI value. To help with this, there is a legend on the map showing these maximum distances (Figure 4.1).

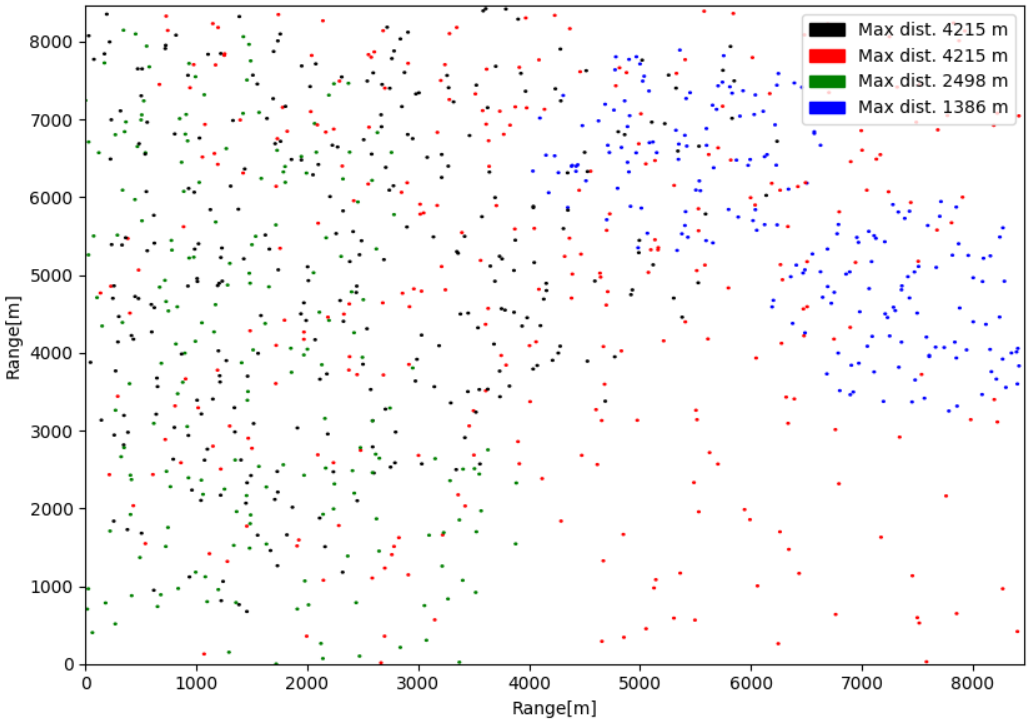

Figure 4.1: Example of LoRa devices disposition.

The simulation process takes a file containing the information about the devices of

the network (number of groups, number of devices per group, mode, payload and average send time between packets) and their respective coordinates (Figure 4.2). Then, the user is prompted to choose the location of the gateway(s) by inserting their coordinates. Finally, the user then chooses the simulation time and the collision model.

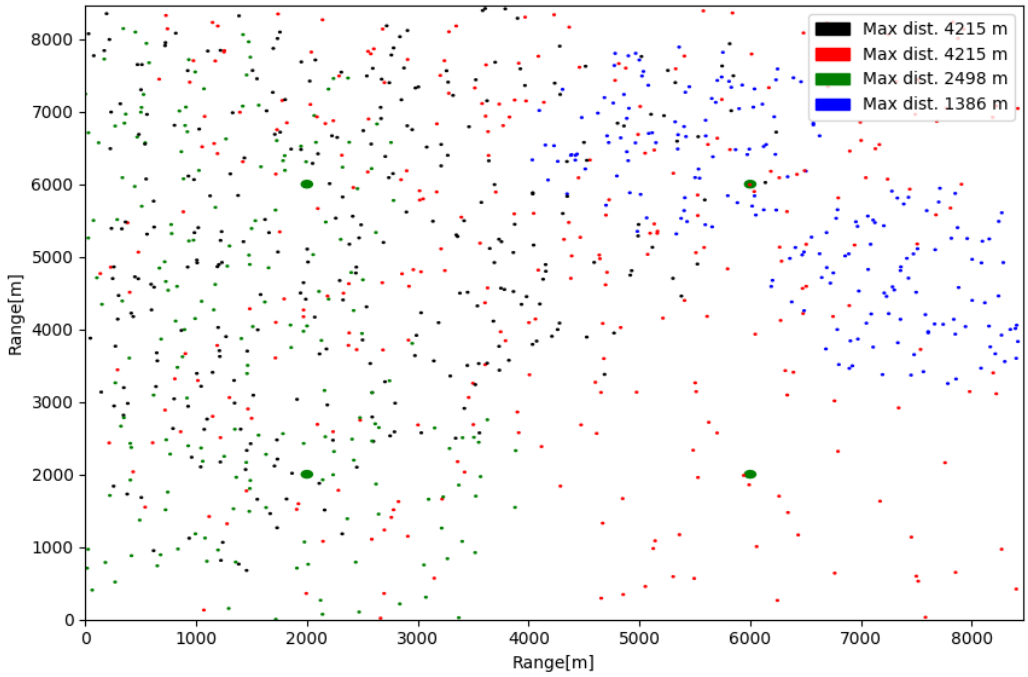

Figure 4.2: Example of LoRa devices disposition with four gateways represented as thick green dots.

4.2 Simulation Results

Initially some simulations are performed with devices of the same DR and different network densities, to analyze the behaviour regarding the gateway placement and the amount of gateways needed to achieve an acceptable DER value. Afterwards, simulations portraying a network with device diversity and its corresponding results are presented. All the simulations are performed with a duty cycle of 1% and a total duration time of 1 hour (3.600.000 *ms*).

4.2.1 Single Mode - Low Network Density

On Figure 4.3 its presented a network with 100 nodes and operating under the mode 3 (Table 4.1). Due to the characteristics of this mode (slow speed, high available distance), there is a broad choice to place the gateways.

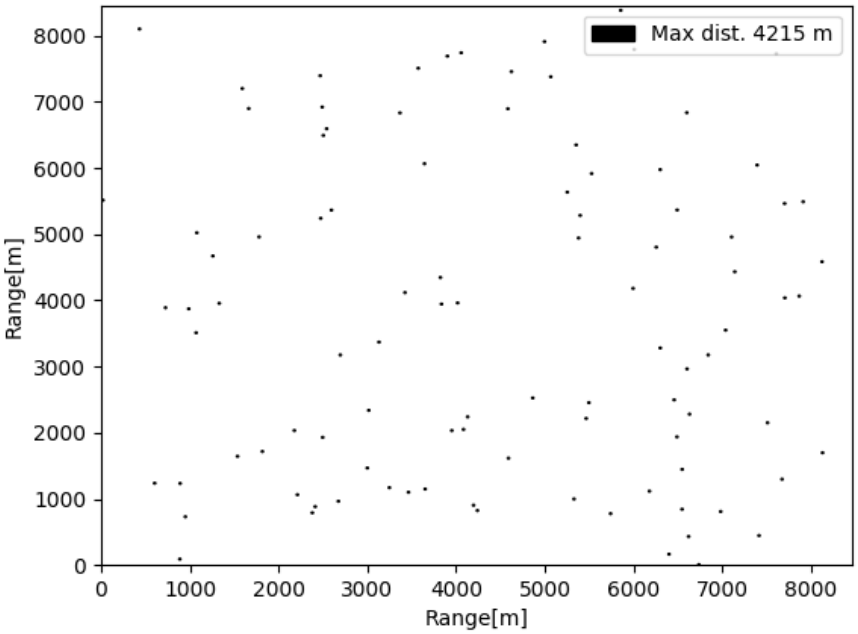

Figure 4.3: LoRa network with 100 devices of the same data rate.

Figure 4.4 shows the same network with one gateway placed at the center of the network. This choice was taken due to the placement of the devices and the maximum distance that these support.

On Table 4.1 its the analysis of this network. As it can be seen, the choice for the gateway placement was appropriate, due to the low number of packets that were lost, meaning that the majority of the nodes are in the communication range to the gateway. However, results show that there is a high amount of collisions on the network, due to the fact that there is no orthogonality among the devices, therefore promoting the collisions of the packets.

Now instead of using a single gateway, three were used. Figure 4.5 shows the placement of the three gateways in the network. The choice of placement was used based on the previous analysis on Table 4.1, which presented a low value for lost packets and a high value for collisions. Therefore, the choice of positioning was more of a concern to mitigate the saturation of the first gateway, than to get more coverage for

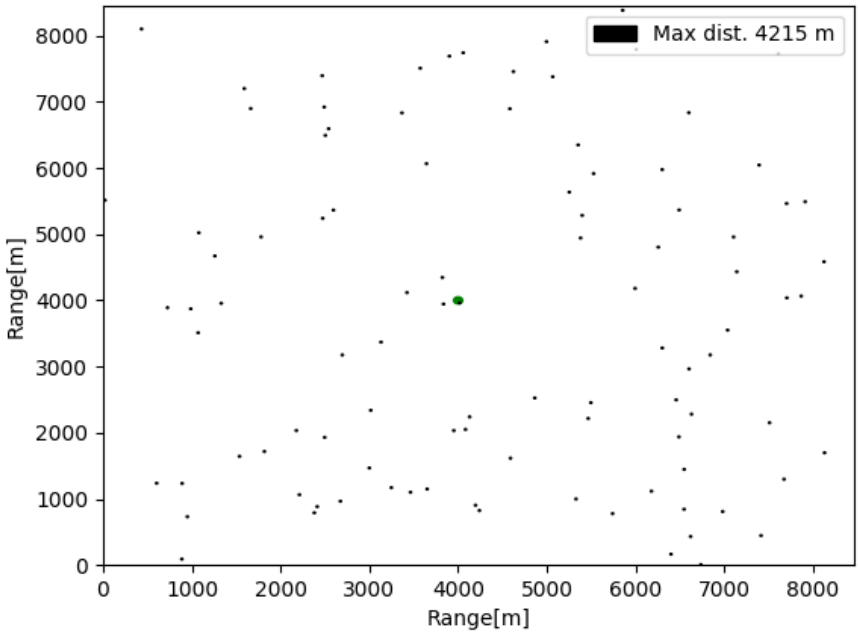

Figure 4.4: LoRa network with 100 devices of the same data rate and 1 gateway.

Table 4.1: Network performance of 100 nodes network with the same data rate and 1 gateway.

	Gateway (x = 4000, y = 4000)
Received Packets	894
Total Collisions	1.254
Lost Packets	58
Sent Packets	2.206
DER	40%

the devices, since the majority of these already reached the first gateway successfully.

Table 4.2 shows the performance of the network with three gateways, as well as some key metrics to evaluate its performance. The distinct sent packets represents the unique packets transmitted. Since each node transmits in broadcast for all the gateways in the network, it is possible that multiple gateways receive the same packet, so this metric allows to see how many distinct packets were transmitted. The distinct received packets show the total unique packets received by the gateways. Distinct lost packets show the amount of packets that did not reach any gateway by not having enough RSSI. Total distinct collisions show the unique packets that were collided in all the gateways.

Finally, the total not received packets metric represent the packets that were not

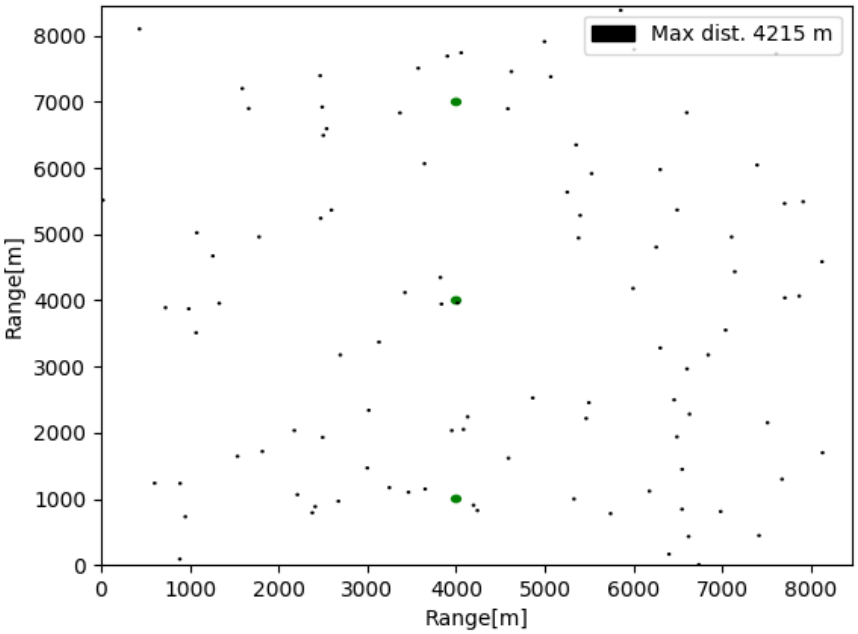

Figure 4.5: LoRa network with 100 devices of the same data rate and 3 gateways.

processed by the gateways, by either colliding or by being lost. This metric is used due to the standard communication method of LoRa, that sends the same packet to all the gateways of the network and relies on the network server to filter these duplicate packets. For instance, if packet 1 was flagged as collided on gateway 1, and lost on the rest of the gateways, this packet is considered as a not received packet.

Table 4.2: Network performance of 100 nodes network with the same data rate and 3 gateways.

	Received Packets
Gateway 1 (x = 4000, y = 4000)	859
Gateway 2 (x = 4000, y = 7000)	611
Gateway 3 (x = 4000, y = 1000)	664
Total Distinct Received Packets	1.294
Total Distinct Sent Packets	2.034
Total Distinct Collisions	218
Total Not Received Packets	522
DER	63 %

As expected, the total distinct received packets increased due to the use of two additional gateways, allowing the packets that were collided in the first gateway to be successfully decoded on gateway 2 and 3. The number of collisions also decreased

due to the addition of the two additional gateways, allowing the packets that were previous collided in gateway 1, to be decoded in either gateway 2 or 3. Results show that there was a increase of 23% of the DER value when comparing both networks.

Progressing on the analysis, this time an additional gateway was introduced, having the total of 4 gateways. Figure 4.6 shows the displacement of the gateways. The previous gateways remained in the same position, while the fourth gateway was placed in a location where the density is higher than the other zones.

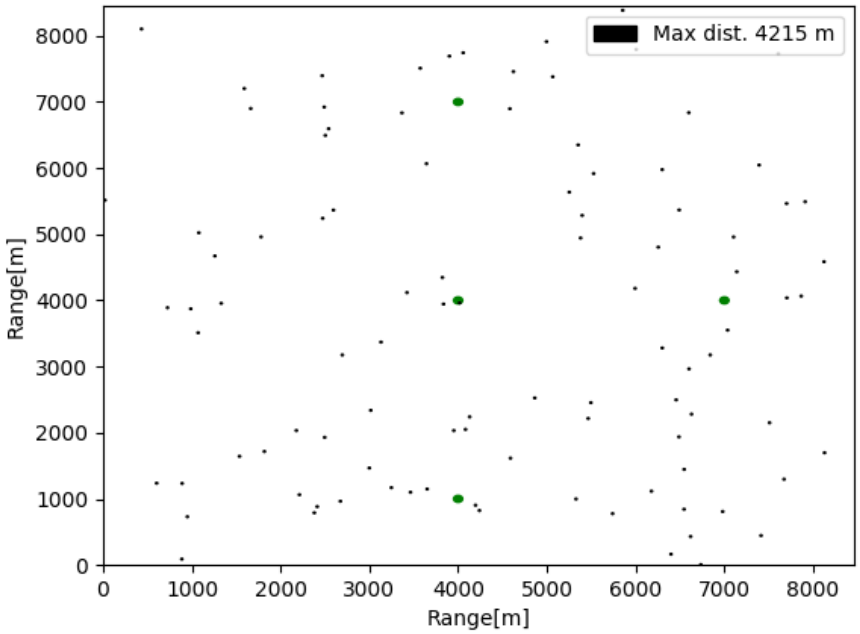

Figure 4.6: LoRa network with 100 devices of the same data rate and 4 gateways.

Table 4.3 shows the results of the network with four gateways. Comparing these results with the results obtained in Table 4.2, the quality of the network did not increase much, as opposed to the increase in network quality obtained when changing from one gateway to three (Tables 4.1 and 4.2).

To prove that the network is near its full potential, an additional gateway was placed. Once again, the previous gateways maintained their positions and the new one was placed in a zone that had a considerable density when compared with others (Figure 4.7).

The performance of the five gateways network is shown on Table 4.4. As expected, there was not a significant change with the additional gateway, showing that the network is already under its maximum capacity with the current choice of modes that the devices operate.

Table 4.3: Network performance of 100 nodes network with the same data rate and 4 gateways.

	Received Packets
Gateway 1 (x = 4000, y = 4000)	903
Gateway 2 (x = 4000, y = 7000)	614
Gateway 3 (x = 4000, y = 1000)	668
Gateway 4 (x = 7000, y = 4000)	689
Total Distinct Received Packets	1.442
Total Distinct Sent Packets	2.121
Total Distinct Collisions	188
Total Not Received Packets	491
DER	68 %

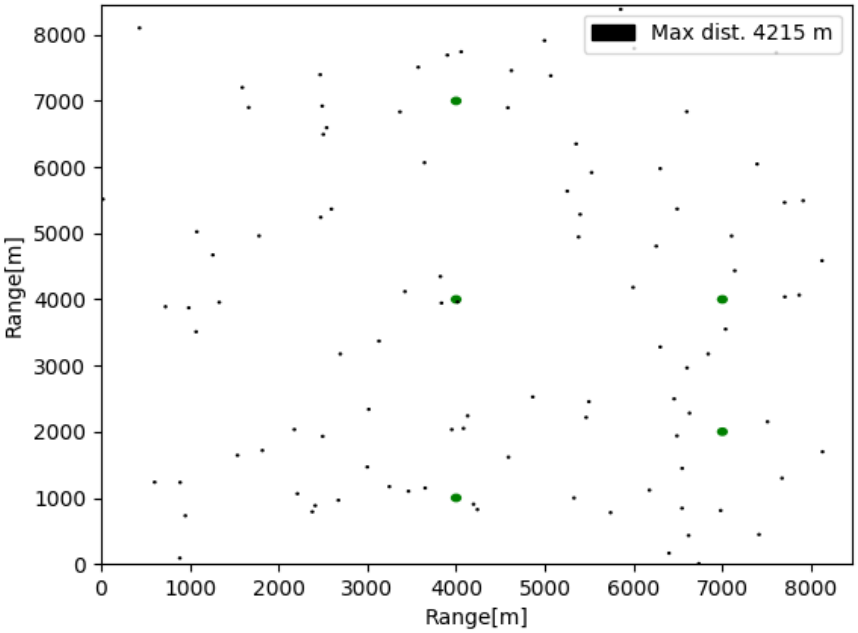

Figure 4.7: LoRa network with 100 devices of the same data rate and 5 gateways.

Table 4.4: Network performance of 100 nodes network with the same data rate and 5 gateways.

	Received Packets
Gateway 1 (x = 4000, y = 4000)	928
Gateway 2 (x = 4000, y = 7000)	590
Gateway 3 (x = 4000, y = 1000)	650
Gateway 4 (x = 7000, y = 4000)	656
Gateway 5 (x = 7000, y = 2000)	560
Total Distinct Received Packets	1.495
Total Distinct Sent Packets	2.167
Total Distinct Collisions	154
Total Not Received Packets	518
DER	69 %

4.2.2 Single Mode - High Network Density

Now the same experiment is done with a higher density network. On Figure 4.8 there is an example of a network with 1000 devices working in the mode 3 (Table 3.4)

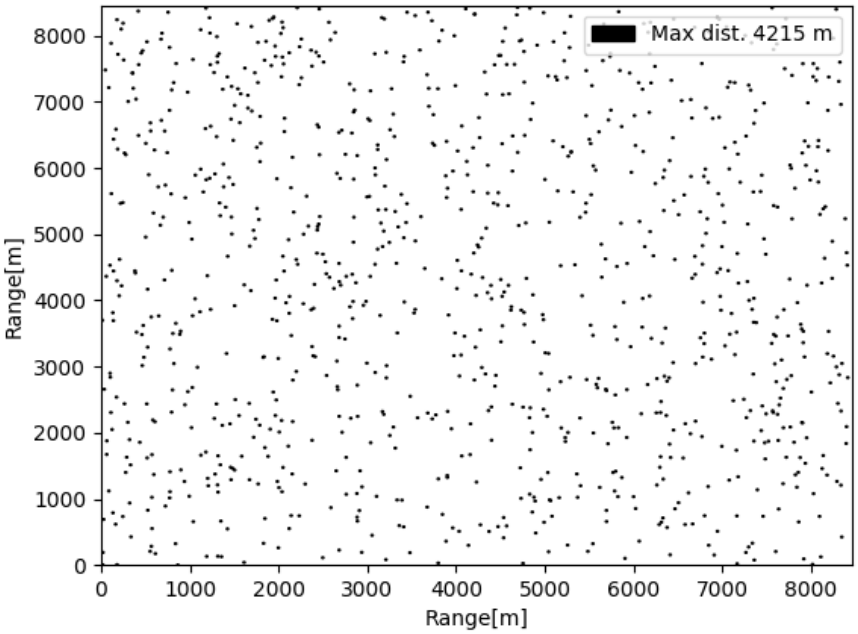

Figure 4.8: LoRa network with 1000 devices of the same data rate.

First, only one gateway is used to simulate this network. Since the devices are randomly placed around the network and given the maximum distance that these devices can reach, the choice to place the gateway in the center of the map is the most logical action (Figure 4.9).

Similarly to the simulations done for the 100 nodes group, since there is only one mode operating in the network, this bear some intricacies to the performance because there is no orthogonality among the devices, therefore promoting the collisions among the packets (Table 4.5). As expected, due to the lack of diversity in operating data rates of the network, the amount of received packets is very low, thus leading to a poor DER value.

Now instead of using only one gateway, five were used and some results were drawn. On Figure 4.10 there is the placement used for all the gateways of the network. Keeping the gateway used in the previous analysis, the other four were placed equidistant to the center gateway with the intent to increase the packet reception.

On Table 4.6 there is the analysis with the performance in this network. As seen

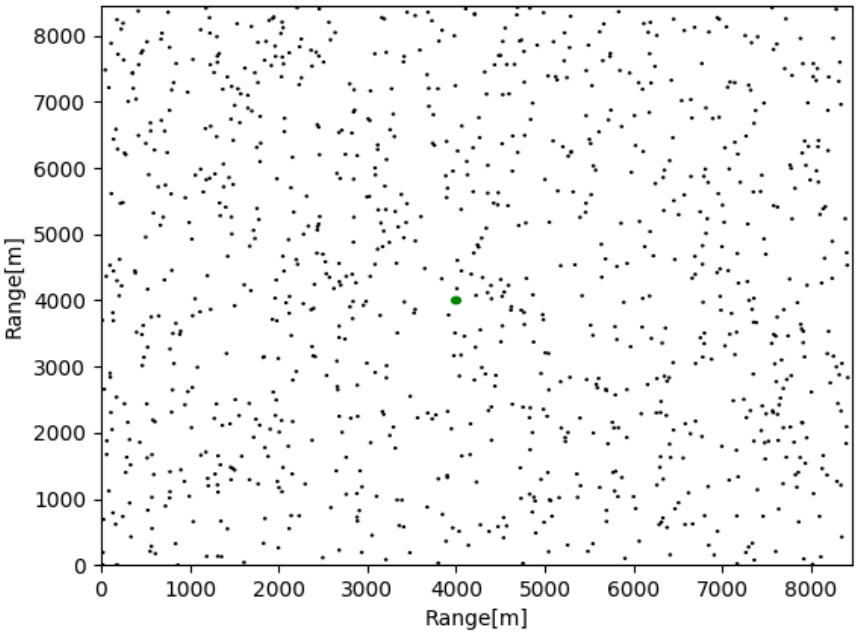

Figure 4.9: LoRa network with 1000 devices of the same data rate and 1 gateway.

Table 4.5: Received packets and DER of the network with 1 data rate and 1 gateway.

	Gateway (x = 4000, y = 4000)
Received Packets	166
Total Collisions	19.617
Lost Packets	1.028
Sent Packets	20.811
DER	0.008 %

by the amount of received packets and respective DER, there was not much change between these two scenarios.

Comparing both results of Tables 4.5 and 4.6, it is noticeable that there is a saturation of the network, as seen by the very slight increase of the DER value. This is due to the use of devices that share the same characteristics among them (DR), not allowing for any kind of orthogonality in the transmission of the packets, as seen by the high number of collisions and packets that were not received. Opposite to the simulations done previously in subsection 4.2.1 with 100 nodes of the same mode, this network failed to present a significant increase of its DER value with the addition of more gateways.

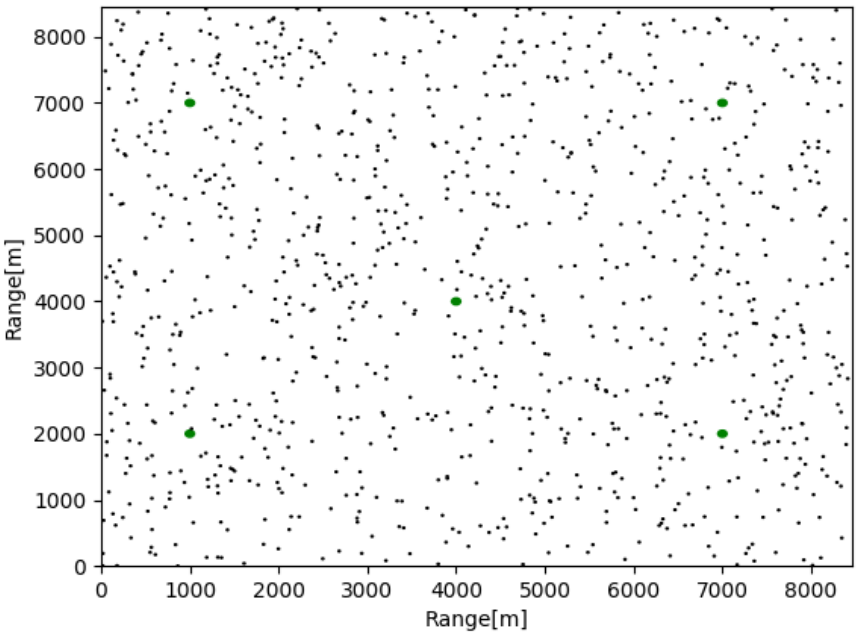

Figure 4.10: LoRa network with 1000 devices of the same data rate and 5 gateways.

Table 4.6: Received packets and DER of the network with 1 data rate and 5 gateways.

	Received Packets
Gateway 1 (x = 4000, y = 4000)	187
Gateway 2 (x = 1000, y = 7000)	12
Gateway 3 (x = 1000, y = 2000)	13
Gateway 4 (x = 7000, y = 7000)	16
Gateway 5 (x = 7000, y = 2000)	21
Total Distinct Received Packets	237
Total Distinct Sent Packets	20.824
Total Distinct Collisions	1.788
Total Not Received Packets	18.799
DER	0.01 %

4.2.3 Multi Mode - Low Network Density

In this subsection an analysis is performed with the behaviour of a low density network with different data rates. On Figure 4.11 there is a network with 100 nodes spread across 10 groups (each group has 10 nodes) and 4 data rates. The configuration of each group is as follows:

- **Group 1 and 10 (blue):**

  Mode: 0

  Payload: 20 Bytes

  Average send time between packets: 1 seconds (1414 *ms*)

- **Group 2 and 8 (green):**

  Mode: 1

  Payload: 20 Bytes

  Average send time between packets: 9 seconds (9267 *ms*)

- **Group 3, 6 and 9 (red):**

  Mode: 2

  Payload: 20 Bytes

  Average send time between packets: 2 minutes and 12 seconds (131891 *ms*)

- **Group 4, 5 and 7 (black):**

  Mode: 3

  Payload: 20 Bytes

  Average send time between packets: 2 minutes and 51 seconds (171213 *ms*)

Since there is a diversity in the characteristics of the devices in this network and due to the low density of devices (which makes for a disperse placement of each device), there is no ideal position to place the gateway, therefore, the center of the network is choice to place the gateway, as seen on Figure 4.12.

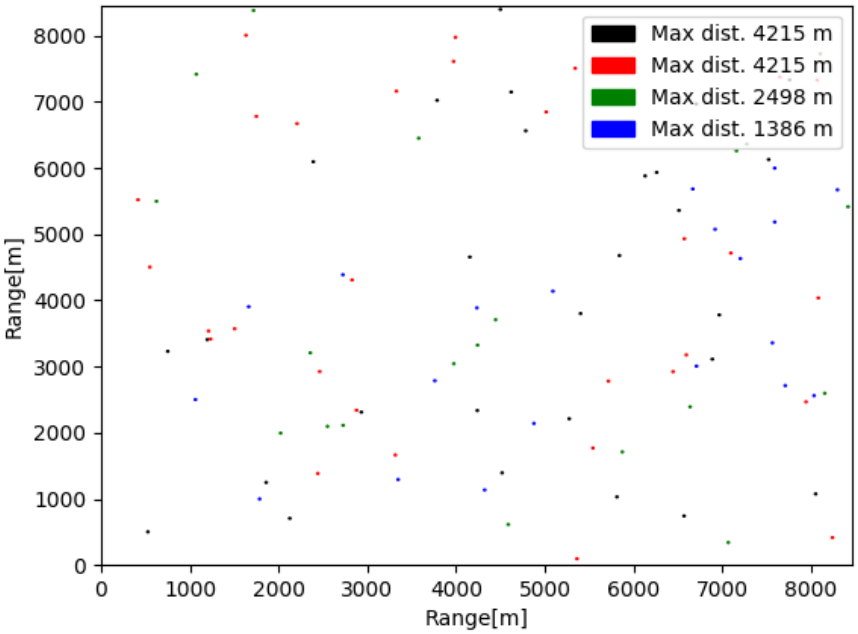

Figure 4.11: LoRa network with 100 devices with different data rates.

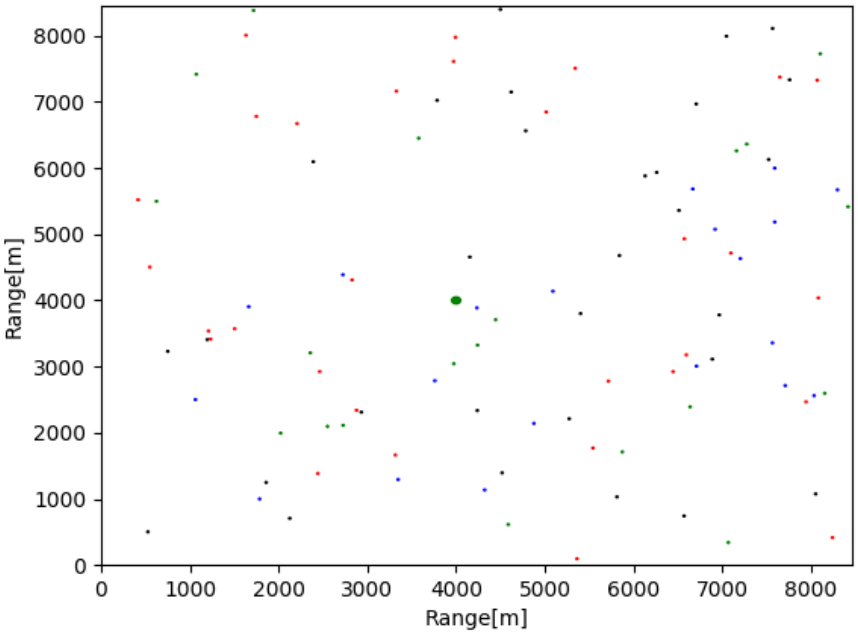

Figure 4.12: LoRa network with 100 devices with different data rates and 1 gateway.

Table 4.7 shows the performance of this network. As expected, there is a poor network performance as seen by the low DER value. This happens because there are

groups that have a high DR, trading shorter transmitting distances for high speed.

Table 4.7: Network performance of 100 nodes network with different data rates and 1 gateway.

	Gateway (x = 4000, y = 4000)
Received Packets	11.730
Total Collisions	2.402
Lost Packets	45.586
Sent Packets	59.718
DER	19,6%

On Table 4.8 there is a breakdown of each group, presenting the amount of received and sent packets as well as the DER value of it. As expected, group 1 is one of the groups that present the lowest value of DER, due to the short distance that supports. Group 10 shares the same DR as group 1, but has a higher DER caused by the better positioning to the gateway. Groups 3, 4, 5, 6, 7 and 9 show the best performance due to their high distance availability, not being much punished by the gateway placement.

Table 4.8: Network performance by group with 1 gateway.

Group	Received Packets	Sent Packets	DER
1 (blue)	0	25.088	0%
2 (green)	688	3.802	18%
3 (red)	157	275	57%
4 (black)	138	211	65%
5 (black)	138	201	69%
6 (red)	244	316	77%
7 (black)	130	215	60%
8 (green)	1.708	3.877	44%
9 (red)	180	264	68%
10 (blue)	8.347	25.469	33%

Similarly to the previous analysis, two additional gateway were placed. As seen by the analysis on Table 4.8, the groups with the lowest DER value are the blue and green ones, so the choice to place the gateways took this insight into consideration (Figure 4.13).

Table 4.9 show the result of the new network. The two additional gateways proved to be efficient, as the DER value increased by 40%.

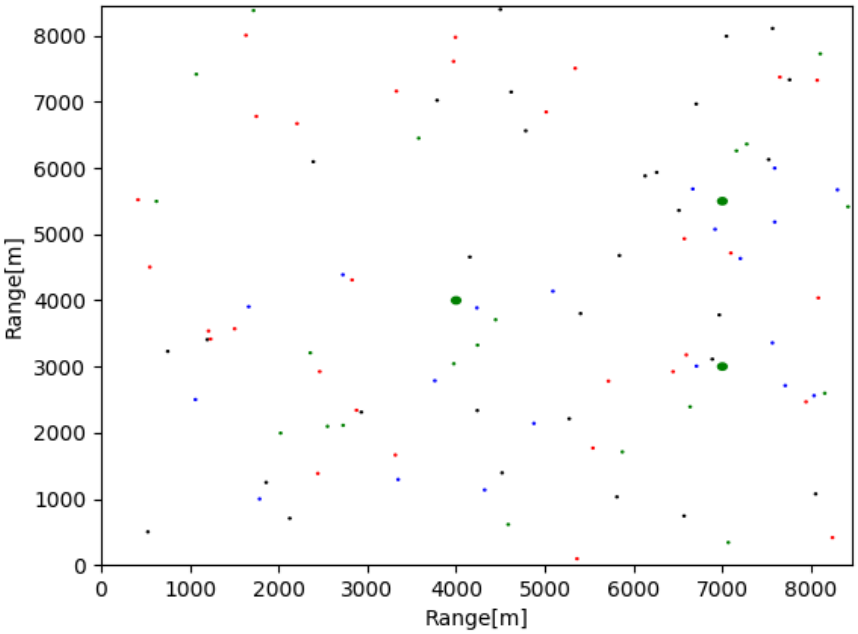

Figure 4.13: LoRa network with 100 devices with different data rates and 3 gateways.

Table 4.9: Network performance of 100 nodes network with different data rates and 3 gateways.

	Received Packets
Gateway 1 (x = 4000, y = 4000)	11.712
Gateway 2 (x = 7000, y = 5500)	14.814
Gateway 3 (x = 7000, y = 3000)	10.175
Total Distinct Received Packets	35.597
Total Distinct Collisions	106
Lost Packets	17.449
Total Not Received Packets	6.385
DER	60 %

Comparing both tables 4.8 and 4.10, the difference in DER for each group increased considerably, where the group 1 and 2 show the greatest enhancement from the additional use of two gateways, as expected by the chosen positioning to place them.

Now an additional gateway was placed, totaling four in the network. The placement for the fourth gateway took into consideration the DER value of the group 10, in an attempt to increase the performance of it (Figure 4.14).

Table 4.10: Network performance by group with 3 gateways.

Group	Received Packets	Sent Packets	DER
1 (blue)	21.332	25.405	84%
2 (green)	2.354	3.824	62%
3 (red)	226	279	81%
4 (black)	159	207	77%
5 (black)	160	194	82%
6 (red)	221	260	85%
7 (black)	169	211	80%
8 (green)	2.340	3.802	62%
9 (red)	217	267	81%
10 (blue)	8.419	25.088	34%

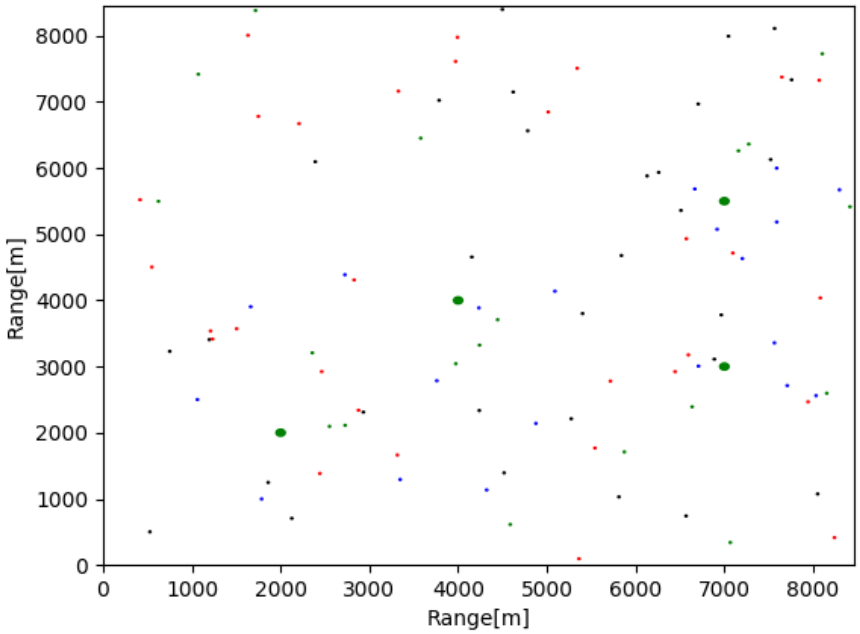

Figure 4.14: LoRa network with 100 devices with different data rates and 4 gateways.

On Table 4.11 it is possible to see that the network performance increased by 8% when compared to the three gateway solution presented on Table 4.9. However, proportionally, the increase of quality from three to four gateways was not as much as the increase from one to three gateways, in resemblance of what as been seen on previous analysis with single mode (4.2.1).

Table 4.12 shows an increase in quality for all the groups of the network, with an emphasize in group 10 where the increase of quality reached the 16%, as expected by

Table 4.11: Network performance of 100 nodes network with different data rates and 4 gateways.

	Received Packets
Gateway 1 (x = 4000, y = 4000)	11.699
Gateway 2 (x = 7000, y = 5500)	14.775
Gateway 3 (x = 7000, y = 3000)	10.133
Gateway 4 (x = 2000, y = 2000)	6.387
Total Distinct Received Packets	40.010
Total Distinct Sent Packets	59.250
Total Distinct Collisions	27
Lost Packets	11.939
Total Not Received Packets	7.274
DER	68 %

the positioning of the new gateway.

Table 4.12: Network performance by group with 4 gateways.

Group	Received Packets	Sent Packets	DER
1 (blue)	21.208	25.215	84%
2 (green)	2.675	3.850	69%
3 (red)	238	287	83%
4 (black)	185	221	84%
5 (black)	197	222	89%
6 (red)	229	264	87%
7 (black)	174	205	85%
8 (green)	2.407	3.867	62%
9 (red)	223	258	86%
10 (blue)	12.474	24.861	50%

However, when looking into the network (Figure 4.11) there are still groups that would benefit from an additional gateway. On Figure 4.15 there is an additional gateway placed in the network, now totaling five. This network will offer coverage to more nodes, where the blue and green modes will benefit more of this new gateway.

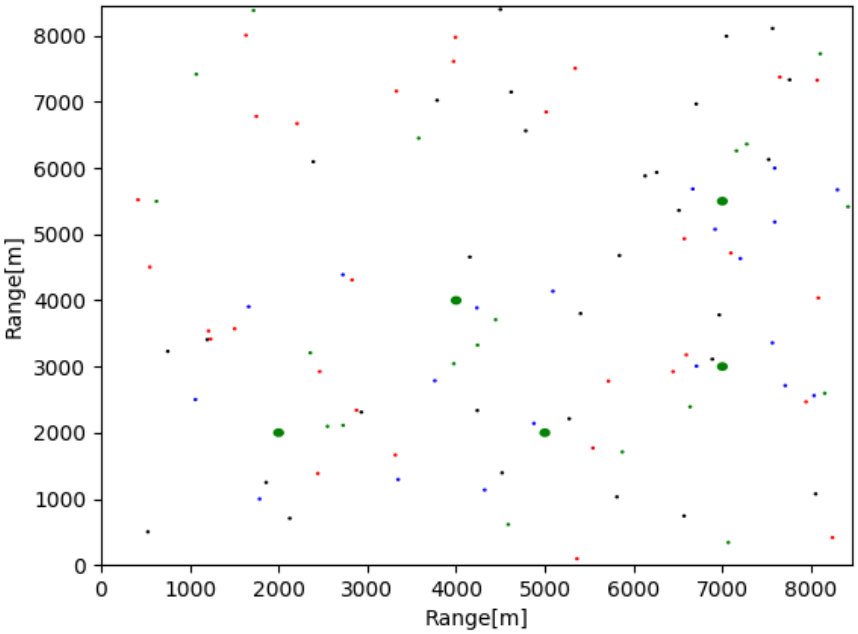

Figure 4.15: LoRa network with 100 devices with different data rates and 5 gateways.

Table 4.13 shows that there was an increase of the DER value of about 7% when compared to the four gateway solution (Table 4.11).

Table 4.13: Network performance of 100 nodes network with different data rates and 5 gateways.

	Received Packets
Gateway 1 (x = 4000, y = 4000)	11.839
Gateway 2 (x = 7000, y = 5500)	14.812
Gateway 3 (x = 7000, y = 3000)	10.165
Gateway 4 (x = 2000, y = 2000)	6.485
Gateway 5 (x = 5000, y = 2000)	7.779
Total Distinct Received Packets	44.943
Total Distinct Sent Packets	59.909
Total Distinct Collisions	48
Lost Packets	6.583
Total Not Received Packets	8.335
DER	75 %

As expected, this gateway brought more performance to the network, namely to the blue and green groups of the network. As seen on Table 4.14, group 2 and 10 were the ones that benefited the most, by having an increase of 9% and 17% respectively, when compared to the previous analysis on Table 4.12.

Table 4.14: Network performance by group with 5 gateways.

Group	Received Packets	Sent Packets	DER
1 (blue)	21.232	25.317	84%
2 (green)	2.986	3.830	78%
3 (red)	223	275	81%
4 (black)	212	244	87%
5 (black)	184	213	86%
6 (red)	252	297	85%
7 (black)	187	220	85%
8 (green)	2.372	3.827	62%
9 (red)	258	291	89%
10 (blue)	17.037	25.395	67%

Going forward in the analysis, since there was an increase of the DER value when increasing the number of gateways up until now, a sixth gateway was added. The position of this gateway was picked due to the amount of devices in that area, being much more crowded than the rest, as seen on Figure 4.16

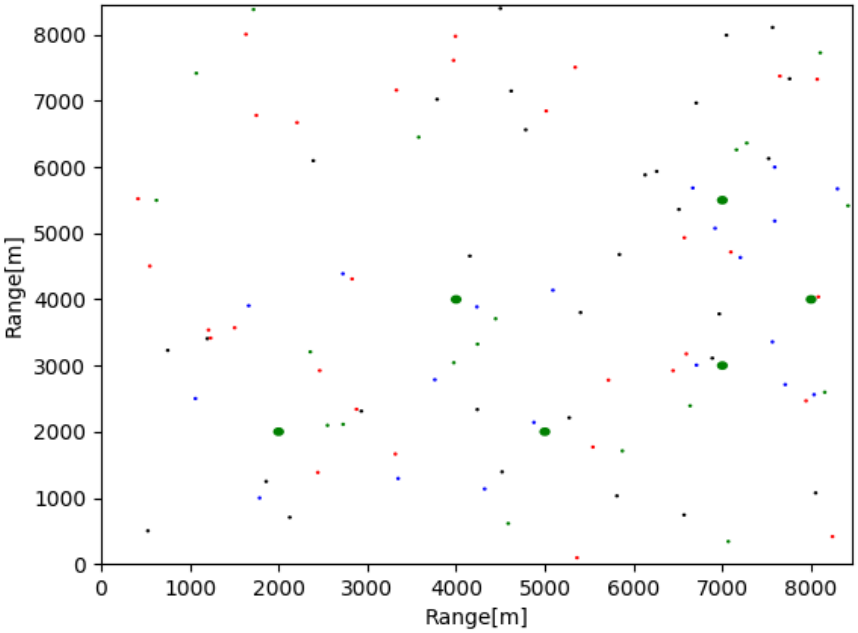

Figure 4.16: LoRa network with 100 devices with different data rates and 6 gateways.

The additional gateway did not prove to be of any use, as seen by the DER value presented on Table 4.15. This means that the network reached its full potential, whereas the increase of the number of gateways from this point forward will not increase the quality of the network, only the cost.

Table 4.15: Network performance of 100 nodes network with different data rates and 6 gateways.

	Received Packets
Gateway 1 (x = 4000, y = 4000)	11.774
Gateway 2 (x = 7000, y = 5500)	14.801
Gateway 3 (x = 7000, y = 3000)	10.121
Gateway 4 (x = 2000, y = 2000)	6.467
Gateway 5 (x = 5000, y = 2000)	7.586
Gateway 6 (x = 8000, y = 4000)	10.710
Total Distinct Received Packets	45.174
Total Distinct Sent Packets	59.707
Total Distinct Collisions	37
Lost Packets	6.564
Total Not Received Packets	7.932
DER	75 %

4.2.4 Multi Mode - High Network Density

In this subsection an analysis is performed with the behaviour of a high density network with different data rates. On Figure 4.17 there is a network with 1000 nodes spread across 10 groups (each with 100 nodes) operating with the 4 data rates of Table 3.4. The configuration of each group is the same as demonstrated on subsection 4.2.3.

As mentioned before, on Figure 4.1 it is possible to see the maximum ranges that each group can achieve. With this information the planning of the network can be made accordingly. Since the fastest DR also have the shortest distance, it is a good practice to place at least one gateway nearby these groups to avoid packet loss. Conversely, those with the slowest DR have the largest distance available and are more flexible concerning gateway placement.

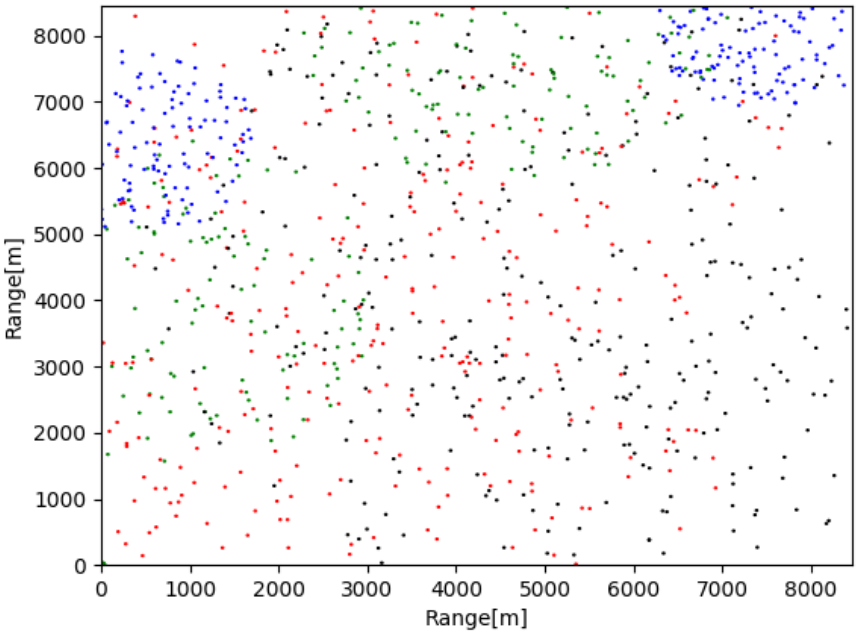

Figure 4.17: LoRa network with 1000 devices with different data rates.

Initially, three gateways were tested in this network: two near the group 1 and 10 and another nearly at the center of the city that will serve the remainder of the groups in the network (Figure 4.18).

Using the non-destructive mode to analyze the results of the network, the performance is seen on Tables 4.16 and 4.17.

On Table 4.16 the total sent packets of the network is presented, along with the amount that each gateway received and the DER value. Analyzing these values, it is

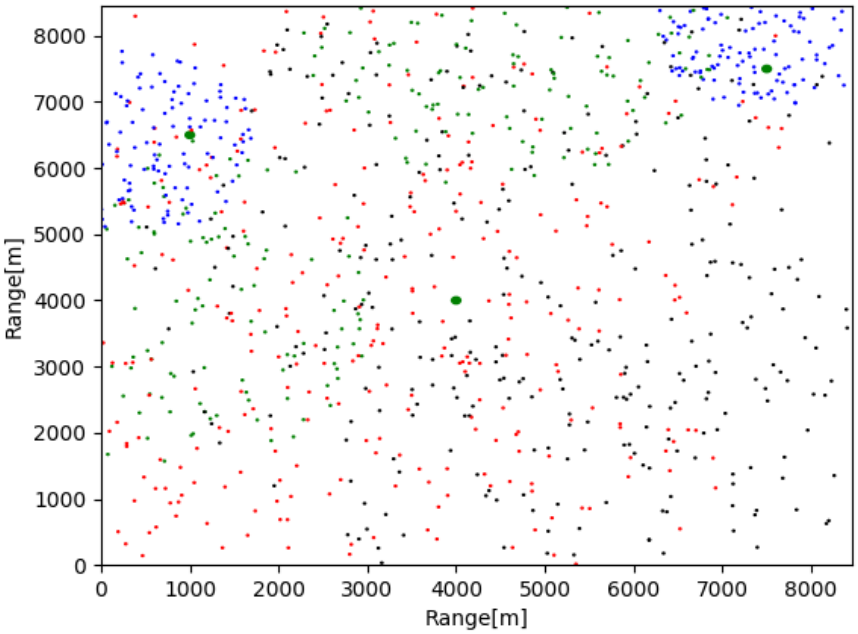

Figure 4.18: LoRa network with 1000 devices with different data rates and 3 gateways.

possible to see that choosing the position for gateway 1 and 2 favored the reception of packets from group 1 and 10, while choosing gateway 3 to serve the rest of the nodes in the network resulted in a lower number of received packets.

Table 4.16: Network performance of 1000 nodes network with different data rates and 3 gateways.

Gateway	Received Packets
Gateway 1 (x = 1000, y = 6500)	85.583
Gateway 2 (x = 7500, y = 7500)	81.431
Gateway 3 (x = 4000, y = 4000)	25.482
Total Distinct Received Packets	177.407
Total Distinct Sent Packets	594.918
Total Distinct Collisions	161
Lost Packets	41.921
Total Not Received Packets	375.429
DER	30 %

Table 4.17 shows the amount of received and sent packets by group. Group 1 and 10, despite having both gateways near them, have the lowest DER value. Group 2 and 8 present the second lowest DER value, mostly because there were packets from these groups that were lost since there was not a wide coverage for these devices. The rest of the groups have the largest amount of distance available, allowing them to reach at

least one gateway in the network, thus having high DER values.

Table 4.17: Network performance by group with 3 gateways.

Group	Received Packets	Sent Packets	DER
1 (blue)	63.560	251.882	25%
2 (green)	20.228	38.343	53%
3 (red)	2.475	2.656	93%
4 (black)	1.880	2.058	91%
5 (black)	1.919	2.058	93%
6 (red)	2.570	2.707	94%
7 (black)	1.907	2.017	95%
8 (green)	19.593	38.401	51%
9 (red)	2.441	2.680	91%
10 (blue)	60.834	252.116	24%

Taking the previous analysis on Table 4.17 that shows the DER value of each group in the network, some arrangements can be considered to increase the network quality. On Figure 4.19 there is the same network but this time with 5 gateways, having 2 more near group 1 and 10. This choice of placement was considered since these areas show a high density of devices and based on the previous analysis on Table 4.17.

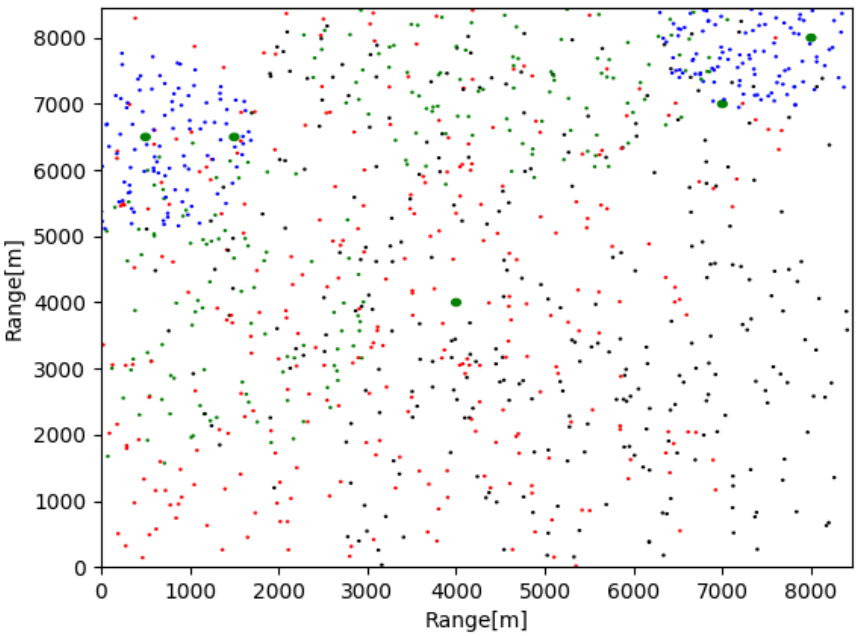

Figure 4.19: LoRa network with 1000 devices with different data rates and 5 gateways.

On Table 4.18 there is the configuration of the 5 gateways network. The increase

of gateways in the network improved the packet reception, as seen by the increase of 5% in the DER value.

Table 4.18: Network performance of 1000 nodes network with different data rates and 5 gateways.

Gateway	Received Packets
Gateway 1 (x = 500, y = 6500)	82.252
Gateway 2 (x = 1500, y = 6500)	76.802
Gateway 3 (x = 7000, y = 7000)	75.857
Gateway 4 (x = 8000, y = 8000)	65.238
Gateway 5 (x = 4000, y = 4000)	25.509
Total Distinct Received Packets	208.968
Total Distinct Sent Packets	595.759
Lost Packets	29.510
Distinct Total Collisions	107
Distinct Not Received Packets	357.174
DER	35 %

Table 4.19 show that the DER value by group varied for groups 1, 10 and 8, as a consequence of adding the two extra gateways. When comparing the results shown in Table 4.16 with Table 4.18, there are some differences worth mentioning. First, the distinct received packets increased, as expected by adding two extra gateways. The lost packets also diminished, showing that the additional gateways provided more coverage to the devices in the network. Concerning the collisions, as seen by the difference of distinct total collisions, there were also less unique collisions between the packets. As a consequence of the network improvement, the amount of packets that were not received by the network also decreased.

Table 4.19: Network performance by group with 5 gateways.

Group	Received Packets	Sent Packets	DER
1 (blue)	75.498	252.228	30%
2 (green)	20.188	38.667	53%
3 (red)	2.535	2.714	93%
4 (black)	1.903	2.052	93%
5 (black)	1.911	2.032	94%
6 (red)	2.482	2.613	95%
7 (black)	1.967	2.086	95%
8 (green)	26.230	38.616	68%
9 (red)	2.379	2.588	92%
10 (blue)	73.875	252.163	29%

Since there was an improve of 5% when going from three to five gateways and there was still margin to enhance the group 1 and 10 reception rate, two more gateways were added to these heavily loaded zones. Figure 4.20 shows the new network with a total of 7 gateways.

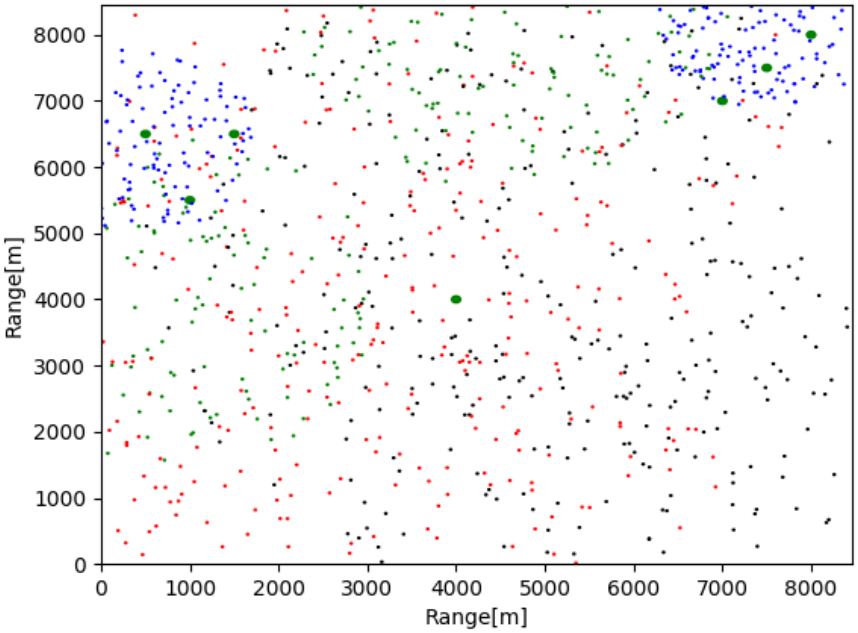

Figure 4.20: LoRa network with 1000 devices with different data rates and 7 gateways.

On table 4.20 there is the overall performance of this network. It is visible that the quality increased by only 3%, as seen by the DER value.

Table 4.21 shows that the targeted groups to improve with the addition of these two gateways hardly changed. Comparing table 4.19 with table 4.21, groups 1 and 10 had an increase of 3% and 4% respectively, while group 2 had the biggest improve of all groups, with 7%.

At this point, its becoming worthless to simply add more gateways to the network, as seen by the continuously small improvement after each addition. In order to obtain a more efficient and with better performance network, the choice, quantity and placement of devices need to be revised, to avoid having high density zones with devices that share the same characteristics. The goal when planning a smart city is to have as much diverse devices as possible by each zone served by a gateway, in order to promote the orthogonality among the devices and therefore increase the odds of each packet being successfully decoded.

Table 4.20: Network performance of 1000 nodes network with different data rates and 5 gateways.

Gateway	Received Packets
Gateway 1 (x = 500, y = 6500)	82.064
Gateway 2 (x = 1500, y = 6500)	76.494
Gateway 3 (x = 7000, y = 7000)	76.193
Gateway 4 (x = 8000, y = 8000)	65.923
Gateway 5 (x = 4000, y = 4000)	25.483
Gateway 6 (x = 1000, y = 5500)	69.035
Gateway 7 (x = 7500, y = 7500)	82.115
Total Distinct Received Packets	228.552
Total Distinct Sent Packets	595.095
Lost Packets	18.037
Distinct Total Collisions	95
Distinct Not Received Packets	348.411
DER	38 %

Table 4.21: Network performance by group with 7 gateways.

Group	Received Packets	Sent Packets	DER
1 (blue)	83.220	252.228	33%
2 (green)	23.349	38.584	60%
3 (red)	2.466	2.648	93%
4 (black)	1.937	2.100	93%
5 (black)	2.024	2.125	95%
6 (red)	2.588	2.727	95%
7 (black)	1.964	2.084	95%
8 (green)	26.279	38.486	68%
9 (red)	2.484	2.695	92%
10 (blue)	82.241	251.418	33%

4.3 Chapter Considerations

This chapter presented an overview of the process steps when trying to emulate the behaviour of a smart city, and the conclusions that can be drawn when choosing the quantity and placement of gateways in the network.

First, an overview of the simulation environment is given, showing the steps to emulate a smart city, by presenting a network planner that generates devices randomly spread around the city, so the user can decide the placement of the gateways.

Then, multiple simulation scenarios are considered to analyze the behaviour of each network. These simulations are split among single mode (where the devices of the network all share the same DR) and multi mode (where the devices are split into groups, each with their own DR). These networks are also evaluated as low density and high density, where the amount of devices vary from 100 to 1000.

Finally, some results were drawn from these analysis. The amount of gateways in the network increase the quality of the network (DER) to some extent. There is a considerable increase in quality when adding more than one gateway to all cases (either low density of high density networks), and the amount of performance gained from increasing the number of gateways decreases with each addition, to the point that there is not any additional benefit from adding more gateways to the network, due to the saturation of devices with the same characteristics (usually with fast DR) that promote packet collision by having no orthogonality shared among them.

5

Conclusions and Future Work

The main goal of this dissertation consisted in improving a widely used LoRa simulator to attend what resembles a real scenario when simulating LoRa networks, and for this reason some additional development was needed.

First, the need of a new propagation model in the simulator that arose from the short communication range the empirical log-distance model (used in the original LoRaSim) had led to take into consideration the choice of a new propagation model. Ultimately, the choice was the Okumura-Hata model. This propagation model was picked because of its widely popularity and efficiency in RF systems applied to urban scenarios, which is one of the focus of this dissertation when analyzing the potential of the simulator once applied to a smart city simulation. Results comparing the empirical propagation model and the Okumura-Hata propagation model have shown that the maximum available distance of the network has significantly increased when using the Okumura-Hata propagation model, leading to a network with more than 40 times the coverage of the original propagation model. This new coverage led to a greater capacity regarding the total devices that the network support and a more dynamic placement of such devices, as the difference in range of communications went from 100 meters to over 4000 meters.

Then, an implementation to an alternative method of the packet collision handler was developed. The destructive nature of pure-ALOHA and the traditionally used 6 dB capture-effect prove to be pessimistic and unrealistic approaches when studying a LoRa network, leading to poor performance networks, specially when looking into

large-scale. For these reasons, the non-destructive approach was implemented. This approach has shown a significant increase in the DER value (20% in the worst case scenario), which translates in a better quality network. Results have shown that the use of this method as a capture-effect is very relevant regardless of the network density, displaying an even higher performance in densely populated scenarios when comparing to the other two (destructive and 6 dB), where the gap among all modes highly favor the non-destructive approach.

Regarding the simulations of a smart city, different scenarios were tested using these changes to the simulator, varying the modes that the devices use and the density of the network. Results have shown that there is a cap to the amount of gateways the network benefits from, because in high density scenarios of devices with the same characteristics the network is already over-strained, and the cost of adding another gateway to these areas do not compensate to the increase in performance gained from it. This is more noticeable in areas where the devices operate in fast mode, promoting the collisions due to the fast data rate and non-orthogonality shared among these devices.

With this work, it is possible to conclude that the Okumura-Hata as a propagation model shows good coverage in a urban scenario and to the IoT landscape is something worth studying into more depth, by applying it into real use-cases and compare them with the results showed in the simulations. The non-destructive approach as a capture-effect allows for a better resources optimization of the networks, as it emphasizes the successful packet reception by dividing each packet RSSI into brackets, and evaluate each case accordingly.

Several features of this work can be enhanced and new ones can be implemented. Some suggestions for future work implementations are the following:

Directive antennas as an option to scenarios where gateway placement is not possible in hot-spots, therefore needing additional RSSI value;

Dynamic data rate calculation based on selected parameters. Instead of calculating the average send time between packets to insert in the simulator, give the option to select the duty cycle, payload and data rate and calculate it respectively;

Network server extension to the network. With the network server module the network can be further optimized, by having the network server to apply the ADR feature (i.e. dynamically adjust the devices parameters based on their distance to the gateway). It would also filter all the duplicated packets generated by the LoRa standard communication.

References

[1] Edith C.-H.Ngai, Bengt Ahlgren, and Markus Hidell, "Internet of Things For Smart Cities: Interoperability and Open Data", *IEEE Internet Computing*, vol. 20, no. 6, 2016.

[2] Xtend IoT, *Top Internet of Things Application Areas*, https://iot.xtendbusiness.com/smart-homes/top-internet-things-application-areas/, [Online; accessed 23-February-2020], 2017.

[3] Alireza Zourmand, Andrew Lai Kun Hing, Chan Wai Hung, and Mohammad AbdulRehman, "Internet of Things (IoT) using LoRa technology", *IEEE International Conference on Automatic Control and Intelligent Systems (I2CACIS)*, 2019.

[4] M. Lauridsen, H. Nguyen, B. Vejlgaard, I. Z. Kovacs, P. Mogensen, and M. Sorensen, "Coverage Comparison of GPRS, NB-IoT, LoRa, and SigFox in a 7800 km^2 Area", in *2017 IEEE 85th Vehicular Technology Conference (VTC Spring)*, 2017, pages 1–5.

[5] LoRaWAN An ns-3 module for simulation of LoRaWAN networks., https://apps.nsnam.org/app/lorawan/, [Online; accessed 2-January-2021].

[6] FLoRa., https://flora.aalto.fi/, [Online; accessed 2-January-2021].

[7] LoRaSim., https://www.lancaster.ac.uk/scc/sites/lora/lorasim.html, [Online; accessed 2-January-2021].

[8] S. Francisco, P. Pinho, and M. Luis, "Improving LoRa Network Simulator for a More Realistic Approach on LoRaWAN ", in *ConfTELE2021*, 2021, pages 1–6.

[9] Jean-Paul Bardyn, Thierry Melly, Olivier Seller, and Nicolas Sornin, "IoT : The Era of LPWAN is starting now", *ESSCIRC Conference 2016: 42nd European Solid-State Circuits Conference*, 2016.

[10] Mohammad Istiak Hossain and Jan Markendahl, "IoT-Communications as a Service: Actor Roles on Indoor Wireless Coverage", *2017 Internet of Things Business Models, Users, and Networks*, 2017.

[11] LoRa, *LoRa Alliance*, https://lora-alliance.org/, [Online; accessed 28-February-2020].

[12] Wi-SUN, https://www.wi-sun.org/, [Online; accessed 28-February-2020].

[13] Sigfox, https://www.sigfox.com/en, [Online; accessed 28-February-2020].

[14] Ingenu, *RPMA Technology*, https://www.ingenu.com/technology/rpma/, [Online; accessed 28-February-2020].

[15] Weightless Technology, http://www.weightless.org/, [Online; accessed 28-February-2020].

[16] DASH7 Alliance, *DASH7*, https://dash7-alliance.org/, [Online; accessed 28-February-2020].

[17] Vodafone NB-IoT, *Specialised Narrowband-IoT services*, https://www.vodafone.com/business/iot/managed-iot-connectivity/nb-iot, [Online; accessed 28-February-2020].

[18] Yasin Kabalcı and Muhammad Ali, "Emerging LPWAN Technologies for Smart Environments: An Outlook", *1st Global Power, Energy and Communication Conference (IEEE GPECOM2019)*, 2019.

[19] IoT Analytics, *Global number of Connected Devices*, https://iot-analytics.com/state-of-the-iot-update-q1-q2-2018-number-of-iot-devices-now-7b/, [Online; accessed 29-February-2020], 2018.

[20] Michael J. McGrath and Cliodhna Ní Scanaill, "Sensor Network Topologies and Design Considerations", in *Sensor Technologies: Healthcare, Wellness, and Environmental Applications*. Berkeley, CA: Apress, 2013, pages 79–95, ISBN: 978-1-4302-6014-1.

[21] Milos-J. Polak L., "Performance analysis of LoRa in the 2.4 GHz ISM band: coexistence issues with Wi-Fi", in *Telecommun Syst 74*. 2020, 299–309.

[22] N. Naik, "LPWAN Technologies for IoT Systems: Choice Between Ultra Narrow Band and Spread Spectrum", in *2018 IEEE International Systems Engineering Symposium (ISSE)*, 2018, pages 1–8.

[23] Dali Ismail, Mahbubur Rahman, and Abusayeed Saifullah, "Low-Power Wide-Area Networks: Opportunities, Challenges, and Directions", in *Proceedings of the Workshop Program of the 19th International Conference on Distributed Computing and Networking*, ser. Workshops ICDCN '18, Varanasi, India: Association for Computing Machinery, 2018, ISBN: 9781450363976.

[24] Alexandros-Apostolos A. Boulogeorgos, Panagiotis D. Diamantoulakis, and George K. Karagiannidis, "Low Power Wide Area Networks (LPWANs) for Internet of Things (IoT) Applications: Research Challenges and Future Trends", *ArXiv*, vol. abs/1611.07449, 2016.

[25] Lorenzo Vangelista, Andrea Zanella, and Michele Zorzi, "Long-Range IoT Technologies: The Dawn of LoRa™", in *1st EAI International Conference on Future access enablers of ubiquitous and intelligent infrastructures*, Sep. 2015, pages 51–58, ISBN: 978-3-319-27071-5.

[26] U. Raza, P. Kulkarni, and M. Sooriyabandara, "Low Power Wide Area Networks: An Overview", *IEEE Communications Surveys Tutorials*, vol. 19, no. 2, pages 855–873, 2017, ISSN: 2373-745X.

[27] E. Shin and G. Jo, "Structure of NB-IoT NodeB system", in *2017 International Conference on Information and Communication Technology Convergence (ICTC)*, 2017, pages 1269–1271.

[28] R. Ratasuk, B. Vejlgaard, N. Mangalvedhe, and A. Ghosh, "NB-IoT system for M2M communication", in *2016 IEEE Wireless Communications and Networking Conference*, 2016, pages 1–5.

[29] N. Mangalvedhe, R. Ratasuk, and A. Ghosh, "NB-IoT deployment study for low power wide area cellular IoT", in *2016 IEEE 27th Annual International Symposium on Personal, Indoor, and Mobile Radio Communications (PIMRC)*, 2016, pages 1–6.

[30] H. Malik, H. Pervaiz, M. Mahtab Alam, Y. Le Moullec, A. Kuusik, and M. Ali Imran, "Radio Resource Management Scheme in NB-IoT Systems", *IEEE Access*, vol. 6, pages 15 051–15 064, 2018, ISSN: 2169-3536.

[31] B. E. Benhiba, A. A. Madi, and A. Addaim, "Comparative Study of The Various new Cellular IoT Technologies", in *2018 International Conference on Electronics, Control, Optimization and Computer Science (ICECOCS)*, 2018, pages 1–4.

[32] R. Ratasuk, D. Bhatoolaul, N. Mangalvedhe, and A. Ghosh, "Performance Analysis of Voice over LTE Using Low-Complexity eMTC Devices", in *2017 IEEE 85th Vehicular Technology Conference (VTC Spring)*, 2017, pages 1–5.

[33] Shancang Li, Li Da Xu, and Shanshan Zhao, "5G Internet of Things: A survey", *Journal of Industrial Information Integration*, vol. 10, pages 1 –9, 2018, ISSN: 2452-414X.

[34] Kais Mekki, Eddy Bajic, Frederic Chaxel, and Fernand Meyer, "A comparative study of LPWAN technologies for large-scale IoT deployment", *ICT Express*, vol. 5, no. 1, pages 1 –7, 2019, ISSN: 2405-9595.

[35] B. Vejlgaard, M. Lauridsen, H. Nguyen, I. Z. Kovacs, P. Mogensen, and M. Sorensen, "Coverage and Capacity Analysis of Sigfox, LoRa, GPRS, and NB-IoT", in *2017 IEEE 85th Vehicular Technology Conference (VTC Spring)*, 2017, pages 1–5.

[36] M. Hata, "Empirical formula for propagation loss in land mobile radio services", *IEEE Transactions on Vehicular Technology*, vol. 29, no. 3, pages 317–325, 1980, ISSN: 1939-9359.

[37] Claire Goursaud and Jean-Marie Gorce, "Dedicated networks for IoT : PHY / MAC state of the art and challenges", *EAI endorsed transactions on Internet of Things*, Oct. 2015.

[38] Ramon Sanchez-Iborra and Maria-Dolores Cano, "State of the Art in LP-WAN Solutions for Industrial IoT Services", *Sensors*, vol. 16, no. 5, 2016, ISSN: 1424-8220.

[39] Nwave, https://www.nwave.io/, [Online; accessed 12-March-2020].

[40] Telensa, https://www.telensa.com/, [Online; accessed 14-March-2020].

[41] W. Ayoub, A. E. Samhat, F. Nouvel, M. Mroue, and J. Prévotet, "Internet of Mobile Things: Overview of LoRaWAN, DASH7, and NB-IoT in LPWANs Standards and Supported Mobility", *IEEE Communications Surveys Tutorials*, vol. 21, no. 2, pages 1561–1581, 2019.

[42] Abusayeed Saifullah, Mahbubur Rahman, Dali Ismail, Chenyang Lu, Ranveer Chandra, and Jie Liu, "SNOW: Sensor Network over White Spaces", Nov. 2016, pages 272–285.

[43] Semtech, https://www.semtech.com/lora, [Online; accessed 16-March-2020].

[44] W. Anani, A. Ouda, and A. Hamou, "A Survey Of Wireless Communications for IoT Echo-Systems", in *2019 IEEE Canadian Conference of Electrical and Computer Engineering (CCECE)*, 2019, pages 1–6.

[45] G. Ferré and A. Giremus, "LoRa Physical Layer Principle and Performance Analysis", in *2018 25th IEEE International Conference on Electronics, Circuits and Systems (ICECS)*, 2018, pages 65–68.

[46] *What are LoRa® and LoRaWAN®?*, https://lora-developers.semtech.com/library/tech-papers-and-guides/lora-and-lorawan/, [Online; accessed 17-March-2021].

[47] Rashmi Sinha, Wei Yiqiao, and Seung-Hoon Hwang, "A survey on LPWA technology: LoRa and NB-IoT", *ICT Express*, vol. 3, Mar. 2017.

[48] M. O. Farooq and D. Pesch, "Analyzing LoRa: A use case perspective", in *2018 IEEE 4th World Forum on Internet of Things (WF-IoT)*, 2018, pages 355–360.

[49] Martin Bor, John Edward Vidler, and Utz Roedig, "LoRa for the Internet of Things", in *EWSN '16 Proceedings of the 2016 International Conference on Embedded Wireless Systems and Networks*, 2016, pages 361–366, ISBN: 9780994988607.

[50] Martin Bor, Utz Roedig, Thiemo Voigt, and Juan Alonso, "Do LoRa low-power wide-area networks scale?", English, in *MSWiM '16 Proceedings of the 19th ACM International Conference on Modeling, Analysis and Simulation of Wireless and Mobile Systems*, ACM Press, Nov. 2016, pages 59–67.

[51] U. Noreen, A. Bounceur, and L. Clavier, "A study of LoRa low power and wide area network technology", in *2017 International Conference on Advanced Technologies for Signal and Image Processing (ATSIP)*, 2017, pages 1–6.

[52] W. Zhou, Z. Tong, Z. Y. Dong, and Y. Wang, "LoRa-Hybrid: A LoRaWAN Based Multihop Solution for Regional Microgrid", in *2019 IEEE 4th International Conference on Computer and Communication Systems (ICCCS)*, 2019, pages 650–654.

[53] S. Sugianto, A. A. Anhar, R. Harwahyu, and R. F. Sari, "Simulation of Mobile LoRa Gateway for Smart Electricity Meter", in *2018 5th International Conference on Electrical Engineering, Computer Science and Informatics (EECSI)*, 2018, pages 292–297.

[54] Aloÿs Augustin, Jiazi Yi, Thomas Heide Clausen, and William Townsley, "A Study of LoRa: Long Range & Low Power Networks for the Internet of Things", *Sensors*, vol. 16, page 1466, Oct. 2016.

[55] Semtech Understanding ADR, https://lora-developers.semtech.com/library/tech-papers-and-guides/understanding-adr/, [Online; accessed 29-March-2020].

[56] P. S. Cheong, J. Bergs, C. Hawinkel, and J. Famaey, "Comparison of LoRaWAN classes and their power consumption", in *2017 IEEE Symposium on Communications and Vehicular Technology (SCVT)*, 2017, pages 1–6.

[57] Mehmet Ali Ertürk, Muhammed Aydın, Talha Büyükakkaşlar, and Hayrettin Evirgen, "A Survey on LoRaWAN Architecture, Protocol and Technologies", *Future Internet*, vol. 11, page 216, Oct. 2019.

[58] N. A. B. Zainal, M. H. Habaebi, I. Chowdhury, and M. R. Islam, "Sensor node clutter distribution in LoRa LPWAN", in *2017 IEEE 4th International Conference on Smart Instrumentation, Measurement and Application (ICSIMA)*, 2017, pages 1–6.

[59] S. Hosseinzadeh, H. Larijani, K. Curtis, A. Wixted, and A. Amini, "Empirical propagation performance evaluation of LoRa for indoor environment", in *2017 IEEE 15th International Conference on Industrial Informatics (INDIN)*, 2017, pages 26–31.

[60] U. Noreen, L. Clavier, and A. Bounceur, "LoRa-like CSS-based PHY layer, Capture Effect and Serial Interference Cancellation", in *European Wireless 2018; 24th European Wireless Conference*, 2018, pages 1–6.

[61] D. Bankov, E. Khorov, and A. Lyakhov, "Mathematical model of LoRaWAN channel access with capture effect", in *2017 IEEE 28th Annual International Symposium on Personal, Indoor, and Mobile Radio Communications (PIMRC)*, 2017, pages 1–5.

[62] L. Beltramelli, A. Mahmood, P. Osterberg, and M. Gidlund, "LoRa beyond ALOHA: An Investigation of Alternative Random Access Protocols", *IEEE Transactions on Industrial Informatics*, pages 1–1, 2020.

[63] R. Fernandes, R. Oliveira, M. Luís, and S. Sargento, "On the Real Capacity of LoRa Networks: The Impact of Non-Destructive Communications", *IEEE Communications Letters*, vol. 23, no. 12, pages 2437–2441, 2019.

[64] T. To and A. Duda, "Simulation of LoRa in NS-3: Improving LoRa Performance with CSMA", in *2018 IEEE International Conference on Communications (ICC)*, 2018, pages 1–7.

[65] M. Slabicki, G. Premsankar, and M. Di Francesco, "Adaptive configuration of lora networks for dense IoT deployments", in *NOMS 2018 - 2018 IEEE/IFIP Network Operations and Management Symposium*, 2018, pages 1–9.

[66] The Things Network, *LoraWAN Bands and Duty Cycle*, https://www.thethingsnetwork.org/docs/lorawan/duty-cycle.html, [Online; accessed 22-June-2020].

[67] A. Waret, M. Kaneko, A. Guitton, and N. El Rachkidy, "LoRa Throughput Analysis With Imperfect Spreading Factor Orthogonality", *IEEE Wireless Communications Letters*, vol. 8, no. 2, pages 408–411, 2019.

[68] C. Caillouet, M. Heusse, and F. Rousseau, "Optimal SF Allocation in LoRaWAN Considering Physical Capture and Imperfect Orthogonality", in *2019 IEEE Global Communications Conference (GLOBECOM)*, 2019, pages 1–6.

[69] Semtech SX1272/73 Datasheet, https://www.semtech.com/products/wireless-rf/lora-transceivers/sx1272, [Online; accessed 30-June-2020].